PHYSICAL REVIEW D **77,** 025005 (2008)

Casimir forces between compact objects: The scalar case

T. Emig,[1,2] N. Graham,[3,4] R. L. Jaffe,[4] and M. Kardar[5]

[1]*Institut für Theoretische Physik, Universität zu Köln, Zülpicher Strasse 77, 50937 Köln, Germany*
[2]*Laboratoire de Physique Théorique et Modèles Statistiques, CNRS UMR 8626, Bât. 100, Université Paris-Sud, 91405 Orsay cedex, France*
[3]*Department of Physics, Middlebury College, Middlebury, Vermont 05753, USA*
[4]*Center for Theoretical Physics, Laboratory for Nuclear Science, and Department of Physics, Massachusetts Institute of Technology, Cambridge, Massachusetts 02139, USA*
[5]*Department of Physics, Massachusetts Institute of Technology, Cambridge, Massachusetts 02139, USA*

(Received 16 October 2007; published 9 January 2008)

We have developed an exact, general method to compute Casimir interactions between a finite number of compact objects of arbitrary shape and separation. Here, we present details of the method for a scalar field to illustrate our approach in its most simple form; the generalization to electromagnetic fields is outlined in Ref. [T. Emig, N. Graham, R. L. Jaffe, and M. Kardar, Phys. Rev. Lett. **99**, 170403 (2007).]. The interaction between the objects is attributed to quantum fluctuations of source distributions on their surfaces, which we decompose in terms of multipoles. A functional integral over the effective action of multipoles gives the resulting interaction. Each object's shape and boundary conditions enter the effective action only through its scattering matrix. Their relative positions enter through universal translation matrices that depend only on field type and spatial dimension. The distinction of our method from the pairwise summation of two-body potentials is elucidated in terms of the scattering processes between three objects. To illustrate the power of the technique, we consider Robin boundary conditions $\phi - \lambda\partial_n\phi = 0$, which interpolate between Dirichlet and Neumann cases as λ is varied. We obtain the interaction between two such spheres analytically in a large separation expansion, and numerically for all separations. The cases of unequal radii and unequal λ are studied. We find sign changes in the force as a function of separation in certain ranges of λ and see deviations from the proximity force approximation even at short separations, most notably for Neumann boundary conditions.

DOI: 10.1103/PhysRevD.77.025005 PACS numbers: 03.70.+k, 42.25.Fx

I. INTRODUCTION

Casimir forces arise when the quantum fluctuations of a scalar, vector, or even fermion field are modified by the presence of static or slowly changing external objects [1]. The objects can be modeled by boundary conditions that they place on the fluctuating field ϕ, by an external field, σ, to which ϕ couples [2], or, in the case of electromagnetism, by a material with space and frequency dependent dielectric and magnetic properties. The Casimir energy is the difference between the energy of the fluctuating field when then objects are present and when the objects are removed to infinite separation.

The advent of precision experimental measurements of Casimir forces [3–8] and the possibility that they can be applied to nanoscale electromechanical devices [9,10] has stimulated interest in developing a practical way to calculate the dependence of Casimir energies on the shapes of the objects. Many geometries have been analyzed over the years, but the case of compact objects has proved rather difficult. In a recent paper [11] we described a new method that makes possible accurate and efficient calculations of Casimir forces and torques between any number of compact objects. The method applies to electromagnetic fields and dielectrics as well as perfect conductors. It also applies to other fields, such as scalar and Dirac, and to any boundary conditions. In this approach, the Casimir energy is given in terms of the fluctuating field's scattering amplitudes from the individual objects, which encode the effects of the shape and boundary conditions. The scattering amplitudes are known analytically in some cases and numerically in others. If the scattering amplitudes are known, then the method can be applied from asymptotically large separation down to separations that are a small fraction of the dimension of the objects. Results at large separations are obtained using low frequency and low angular momentum expansions of scattering amplitudes. The coefficients multiplying the successive orders in inverse separation can be identified with increasingly detailed characteristics of the objects. At small separations the manipulation of large matrices, whose dimensions grow with angular momentum, eventually slows down the calculation. However at these distances other methods, notably the ''proximity force approximation'' (PFA), apply. Thus it is now possible to obtain an understanding of Casimir forces and torques at all separations for compact objects and to compute the explicit form of the interaction if the scattering matrices of the individual objects are available [12–14].

The aim of this paper is to provide a pedagogical introduction to our methods by treating in detail the simplest case, a scalar field obeying a boundary condition on a sharp surface. The complications of electromagnetism and smoothly varying dielectrics were already introduced briefly in Ref. [11]. They will be treated in more detail in

subsequent publications [15]. Our approach relies on a marriage of methods from path integral and scattering formalisms, so we provide background on both of these subjects as they apply to Casimir effects.

Schwinger, in particular, emphasized that Casimir forces could be understood as ordinary electromagnetic interactions between quantum fluctuations of charge and current in metals or dielectrics [16]. We implement this idea here through a functional integral formulation. We begin by writing the Casimir energy as the logarithm of a functional integral over all field fluctuations constrained by the boundary conditions on a set of surfaces. Following Refs. [17,18] we implement the boundary conditions by introducing integrals over sources that enforce the boundary conditions as functional δ-functions. Next we perform the functional integral over the field. The result is an integral of the form $\prod_\alpha \int \mathcal{D}\varrho_\alpha \exp(iS[\varrho])$, where ϱ_α are the sources on the different surfaces labeled by α and $S[\varrho]$ is the classical action of the field, which is uniquely determined by the sources ϱ_α. The contributions to $S[\varrho]$ are of two qualitatively different forms, those involving sources on different surfaces and those coupling a particular surface source to itself through the field it generates. Both have simple representations in a basis of angular momentum eigenstates ("partial waves") and multipole moments of the sources. The couplings between different objects involve only a well-known kinematic "translation matrix," $\mathbb{U}$, that relates a partial wave amplitude generated by one source to partial waves seen by another [19]. The self-interactions depend only on the "transition matrix," $\mathbb{T}$, (related to the scattering matrix, $\mathbb{S}$, by $\mathbb{T} = \frac{1}{2}(\mathbb{S} - \mathbb{I})$]) [21], which describes the response of the scalar field to the boundary condition on the surface. The result is remarkably simple. For a complex scalar field in the presence of two objects it takes the form,

$$\mathcal{E}_{12}[\mathcal{C}] = \frac{\hbar c}{\pi} \int_0^\infty d\kappa \ln \det(\mathbb{I} - \mathbb{T}^1 \mathbb{U}^{12} \mathbb{T}^2 \mathbb{U}^{21}), \qquad (1.1)$$

where the determinant is over the partial wave indices on the matrices $\mathbb{T}^\alpha$ and $\mathbb{U}^{\alpha\beta}$ and the integral is over $\kappa = -i\omega/c$, the imaginary wave number. In Sec. IV the usefulness of this result is demonstrated through several specific applications.

Casimir forces between compact objects were first considered by Casimir and Polder in 1948 [22]. Since then, two threads of work related to ours have been pursued: attempts to evaluate the Casimir force between compact objects explicitly, and efforts to develop a general framework similar to that embodied in Eq. (1.1). Until recently work along the first line consisted of expansions at asymptotically large separation. Casimir and Polder found the electromagnetic force between two neutral but polarizable atoms to leading order at large separation [22]. Feinberg and Sucher [23] generalized to arbitrary compact objects and included magnetic effects. Balian and Duplantier studied perfect metals, and derived explicit results to leading order at asymptotically large separation [24]. More recently Gies *et al.* [25] used numerical methods to evaluate the Casimir force between two Dirichlet spheres for a scalar field, over a range of subasymptotic separations, and in other open geometries such as a plate and a cylinder [26] or finite plates with edges [27]. Bulgac and collaborators [28] applied scattering theory methods to the same scalar Dirichlet problem and obtained results over a wide range of separations. The only explicit calculations for subasymptotic distances up to now have been for a scalar field obeying Dirichlet boundary conditions on two spheres, a sphere and a plate [28] and for electromagnetic fields for a plate and a cylinder [29,30] and two perfectly conducting spheres [11].

Formulas for the Casimir energy closely related to Eq. (1.1) have appeared previously in the literature. The first appearance we are aware of is in the work of Balian and Duplantier [24] based on the multiple reflection expansion (MRE). Their Eq. (7.20) gives a quantity, Ψ, that is directly related to the Casimir energy, and could form the basis for an approach like ours. Their approach, like ours, punctuates periods of propagation in the vicinity of each object with free propagation between the objects. However no explicit expressions for the propagation kernels, K_α, are given. More recently "log-det" formulas like ours have arisen in several functional integral studies of Casimir forces [29,31]. To our knowledge Kenneth and Klich in Ref. [32] were the first to identify the inverted Green's function as a $\mathbb{T}$-matrix and derive Eq. (1.1) as a formal result. Here also, no explicit form for the matrices was derived. Their derivation applies to scalar fields in a medium with a space and frequency dependent speed of light. For the case of a scalar field, our result can be viewed as an explicit expression for their formula in a basis of partial waves, which we show is particularly well suited to practical applications. Our new derivation of Eq. (1.1) in terms of quantum fluctuations of sources has the advantage that it allows for a physically transparent extension to gauge fields in the presence of material objects with general dielectric and magnetic properties, as outlined in Ref. [11].

In Sec. IV, we provide a number of examples where our approach yields straightforward results for Casimir interactions that could not be obtained before. We carry out explicit analytical and numerical computations for spheres with Robin boundary conditions $\phi - \lambda \partial_n \phi = 0$. The sign of the Casimir interaction at asymptotically large and small distances is classified as a function of the value of the Robin parameter λ. The Casimir energy at asymptotically large separations is obtained as a series in the ratio of distance to sphere radius. We also perform numerical computations of the Casimir interaction of two spheres with Robin boundary conditions spanning the full range of separations, including very short distances, where our results confirm the proximity force approximation (PFA).

At intermediate distances considerable deviations from the PFA are found. For certain values of λ, the Casimir force can change sign (once or twice) as function of separation.

Finally, in Sec. IV D, we give an expression for the Casimir interaction at large separations between two compact object of arbitrary shape and with arbitrary boundary conditions in terms of generalized capacitance coefficients. Technical derivations are presented in three appendices.

II. FOUNDATIONS

In this section we review formalism essential for our work. We use both functional integral methods and techniques originating in scattering theory. First, in Sec. II A we introduce the functional integral approach of Refs. [18,33,34], which allows us to trade the problem of fields fluctuating in the bulk for the interactions of sources defined only on the bounding surfaces. In our approach, individual objects are characterized by the way they scatter the fluctuating fields. This information is summarized in the transition matrix, $\mathbb{T}$, which we introduce in Sec. II B and relate to scattering solutions of the equations of motion and to Green's functions. In the $k \to 0$ limit, Helmholtz's equation reduces to Laplace's equation. In this limit the $\mathbb{T}$-matrix can be related to generalized coefficients of capacitance, which we summarize in Sec. II C. Finally in Sec. II D we introduce the translation formulas that relate partial waves computed with respect to one origin to those computed with respect to another.

A. Functional integral formulation

We consider a complex quantum field, $\phi(\mathbf{x}, t)$, which is defined over all space and constrained by boundary conditions $\mathcal{C}$ on a set of fixed surfaces Σ_α, for $\alpha = 1, 2, \ldots, N$, but is otherwise noninteracting. We assume that the surfaces are closed and compact and refer to their interiors as "objects." Our starting point is the functional integral representation for the trace of the propagator, $\mathrm{Tr} e^{-iH_C T/\hbar}$ [35],

$$\mathrm{Tr}\, e^{-iH_C T/\hbar} = \int [\mathcal{D}\phi]_{\mathcal{C}} e^{(i/\hbar)S[\phi]} \equiv Z[\mathcal{C}], \tag{2.1}$$

where the subscript $\mathcal{C}$ denotes the constraints imposed by the boundary conditions.[1] The integral is over all field configurations that obey the boundary conditions and are periodic in a time interval T. $S[\phi]$ is the action for a free complex field,

$$S[\phi] = \int_0^T dt \int d\mathbf{x} \left(\frac{1}{c^2} |\partial_t \phi|^2 - |\nabla \phi|^2 \right), \tag{2.2}$$

where the $\mathbf{x}$-integration covers all space.[2]

The ground state energy can be projected out of the trace in Eq. (2.1) by setting $T = -i\Lambda/c$ taking the limit $\Lambda \to \infty$,

$$\mathcal{E}_0[\mathcal{C}] = -\lim_{\Lambda\to\infty} \frac{\hbar c}{\Lambda} \ln(\mathrm{Tr} e^{-H_C \Lambda/\hbar c}) = -\lim_{\Lambda\to\infty} \frac{\hbar c}{\Lambda} \ln Z[\mathcal{C}], \tag{2.3}$$

and the Casimir energy is obtained by subtracting the ground state energy when the objects have been removed to infinite separation,

$$\mathcal{E}[\mathcal{C}] = -\lim_{\Lambda\to\infty} \frac{\hbar c}{\Lambda} \ln(Z[\mathcal{C}]/Z_\infty). \tag{2.4}$$

In the standard formulation, the constraints are implemented by boundary conditions on the field ϕ at the surfaces $\{\Sigma_\alpha\}$. The usual choices are Dirichlet, $\phi = 0$, Neumann, $\partial_n \phi = 0$, or mixed (Robin), $\phi - \lambda \partial_n \phi = 0$, where ∂_n is the normal derivative pointing out of the objects. To be specific, we first consider Dirichlet boundary conditions. The extension to the Neumann case is presented in Appendix A. As noted in the Introduction, the only effect of the choice of boundary conditions is to determine which $\mathbb{T}$-matrix appears in the functional determinant, Eq. (1.1).

For readers who are not familiar with the functional integral representation of the Casimir energy, Eq. (2.4), in Appendix B we show that Eq. (2.4) agrees with the traditional definition of the Casimir energy in terms of zero-point energies of normal modes.

Since the constraints on ϕ are time independent, the integral over $\phi(\mathbf{x}, t)$ may be written as an infinite product of integrals over Fourier components,

$$\int [\mathcal{D}\phi]_{\mathcal{C}} = \prod_{n=-\infty}^{\infty} [\mathcal{D}\phi_n(\mathbf{x})]_{\mathcal{C}}, \tag{2.5}$$

where

$$\phi(\mathbf{x}, t) = \sum_{n=-\infty}^{\infty} \phi_n(\mathbf{x}) e^{2\pi i n t/T}, \tag{2.6}$$

and the logarithm of Z becomes a sum,

[1] We have used an abbreviated notation for the functional integral. Since ϕ is complex $\int \mathcal{D}\phi$ should be understood as $\int \mathcal{D}\phi \mathcal{D}\phi^*$, and similarly in subsequent functional integrals.

[2] Note that ϕ is defined and can fluctuate inside the objects bounded by the surfaces Σ_α. In this feature our formalism departs from some treatments where the field is defined to be strictly zero (for Dirichlet boundary conditions) inside the objects. The fluctuations interior to the objects do not depend on the separations between them and therefore do not affect Casimir forces or torques.

$$\ln Z[\mathcal{C}] = \sum_{n=-\infty}^{\infty} \ln\Bigg\{\int [\mathcal{D}\phi_n(\mathbf{x})]_{\mathcal{C}} \exp\Bigg[i\frac{T}{\hbar} \times \int d\mathbf{x}\left(\left(\frac{2\pi n}{cT}\right)^2 |\phi_n(\mathbf{x})|^2 - |\nabla\phi_n(\mathbf{x})|^2\right)\Bigg]\Bigg\}. \tag{2.7}$$

As $T \to \infty$, $\sum_n$ can be replaced by $\frac{cT}{2\pi}\int_{-\infty}^{\infty} dk$, where $k = 2\pi n/(cT)$ and $\phi_n(\mathbf{x})$ is replaced by $\phi(\mathbf{x}, k)$. Combining the positive and negative k-integrals gives

$$\begin{aligned}\ln Z[\mathcal{C}] &= \frac{cT}{\pi}\int_0^{\infty} dk \ln\Bigg\{\int [\mathcal{D}\phi(\mathbf{x}, k)]_{\mathcal{C}} \\ &\quad\times \exp\Bigg[i\frac{T}{\hbar}\int d\mathbf{x}(k^2|\phi(\mathbf{x}, k)|^2 - |\nabla\phi(\mathbf{x}, k)|^2)\Bigg]\Bigg\} \\ &= \frac{cT}{\pi}\int_0^{\infty} dk \ln \beth_{\mathcal{C}}(k),\end{aligned} \tag{2.8}$$

where

$$\beth_{\mathcal{C}}(k) = \int [\mathcal{D}\phi(\mathbf{x}, k)]_{\mathcal{C}} \exp\Bigg[i\frac{T}{\hbar}\int d\mathbf{x}(k^2|\phi(\mathbf{x}, k)|^2 - |\nabla\phi(\mathbf{x}, k)|^2)\Bigg], \tag{2.9}$$

is the functional integral at fixed k.

To extract the Casimir energy, we use $T = -i\Lambda/c$ and Wick rotate the k-integration ($k = i\kappa$ with $\kappa > 0$).[3] Using Eq. (2.4), we obtain,

$$\mathcal{E}[\mathcal{C}] = -\frac{\hbar c}{\pi}\int_0^{\infty} d\kappa \ln\frac{\beth_{\mathcal{C}}(i\kappa)}{\beth_{\infty}(i\kappa)}. \tag{2.10}$$

Here $\beth_{\mathcal{C}}(i\kappa)$ is given by the Euclidean functional integral,

$$\beth_{\mathcal{C}}(i\kappa) = \int [\mathcal{D}\phi(\mathbf{x}, i\kappa)]_{\mathcal{C}} \exp\Bigg[-\frac{T}{\hbar}\int d\mathbf{x}(\kappa^2|\phi(\mathbf{x}, i\kappa)|^2 + |\nabla\phi(\mathbf{x}, i\kappa)|^2)\Bigg]. \tag{2.11}$$

It remains to incorporate the constraints directly into the functional integral using the methods of Refs. [17,18]. Working in Minkowski space, we consider the fixed frequency functional integral, $\beth_{\mathcal{C}}(k)$ (and suppress the label k on the field ϕ). Following Ref. [17,18], we implement the constraints in the functional integral by means of a functional δ-function. For Dirichlet boundary conditions the constraint reads,

$$\int [\mathcal{D}\phi(\mathbf{x})]_{\mathcal{C}} = \int [\mathcal{D}\phi(\mathbf{x})]\prod_{\alpha=1}^{N}\int [\mathcal{D}\varrho_\alpha(\mathbf{x})] \times \exp\Bigg[i\frac{T}{\hbar}\int_{\Sigma_\alpha} d\mathbf{x}(\varrho_\alpha^*(\mathbf{x})\phi(\mathbf{x}) + \text{c.c.})\Bigg], \tag{2.12}$$

where the functional integration over ϕ is no longer constrained. Other boundary conditions can be implemented similarly. In the resulting functional integral,

$$\begin{aligned}\beth_{\mathcal{C}}(k) &= \prod_{\alpha=1}^{N}\int [\mathcal{D}\varrho_\alpha(\mathbf{x})]\int [\mathcal{D}\phi(\mathbf{x})] \\ &\quad\times \exp\Bigg[i\frac{T}{\hbar}\Bigg(\int d\mathbf{x}(k^2|\phi(\mathbf{x})|^2 - |\nabla\phi(\mathbf{x})|^2) \\ &\quad + \sum_\alpha \int_{\Sigma_\alpha} d\mathbf{x}(\varrho_\alpha^*(\mathbf{x})\phi(\mathbf{x}) + \text{c.c.})\Bigg)\Bigg] \\ &\equiv \prod_{\alpha=1}^{N}\int [\mathcal{D}\varrho_\alpha(\mathbf{x})]\int [\mathcal{D}\phi(\mathbf{x})] \exp\left(i\frac{T}{\hbar}\tilde{S}[\phi, \varrho]\right),\end{aligned} \tag{2.13}$$

the fields fluctuate without constraint throughout space and the sources $\{\varrho_\alpha\}$ fluctuate on the surfaces. We denote the new "effective action" including both the fields and sources by $\tilde{S}[\phi, \varrho]$.

B. The scattering amplitude

In this section we consider each of the objects in isolation, and review the solution to the Helmholtz equation

$$-(\nabla^2 + k^2)\phi_\alpha(\mathbf{x}) = 0, \tag{2.14}$$

in the domain *outside* Σ_α. We assume that ϕ_α obeys the Dirichlet boundary condition on Σ_α. It is convenient to fix an origin, $\mathcal{O}_\alpha$, at some point inside the object and introduce a coordinate vector, $\mathbf{x}_\alpha$, defined with respect to this origin. A specific choice of the origin will be made later to simplify the analysis. For simplicity we suppress the label α from now on in this section. We introduce spherical polar coordinates relative to this origin, $r \equiv |\mathbf{x}|$ and $\hat{\mathbf{x}}$. Outside Σ, ϕ is a superposition of partial waves with definite angular momentum,

$$\phi(\mathbf{x}) = \sum_{lm}[c_{lm}h_l^{(2)}(kr) + d_{lm}h_l^{(1)}(kr)]Y_{lm}(\hat{\mathbf{x}}), \tag{2.15}$$

where the spherical Hankel functions, $h_l^{(1)}(kr)$ and $h_l^{(2)}(kr)$ are the outgoing (asymptotic to e^{ikr}/kr) and incoming (asymptotic to e^{-ikr}/kr) solutions, respectively. To make contact with traditional methods of scattering theory, we rewrite $\phi(\mathbf{x})$ in terms of solutions with unit incoming amplitude,

$$\phi(\mathbf{x}) = \sum_{lm} c_{lm}\phi_{lm}(\mathbf{x}), \tag{2.16}$$

where

$$\phi_{lm}(\mathbf{x}) = h_l^{(2)}(kr)Y_{lm}(\hat{\mathbf{x}}) + \sum_{l'm'}\mathcal{S}_{l'm'lm}(k)h_{l'}^{(1)}(kr)Y_{l'm'}(\hat{\mathbf{x}}). \tag{2.17}$$

The coefficients $\mathcal{S}_{lml'm'}(k)$ measure the response of the object, Σ, to a unit amplitude incoming wave with angular

[3] A more careful treatment of the rotation of the integration contour to the imaginary axis is necessary in the presence of bound states.

momentum (lm). They are the matrix elements of the scattering operator, or $\mathbb{S}$-matrix,

$$\mathcal{S}_{l'm'lm}(k) = \langle l'm'|\mathbb{S}(k)|lm\rangle, \tag{2.18}$$

which are fixed by the condition that the resulting basis functions, ϕ_{lm} vanish on Σ. With the object absent, $\mathbb{S}$ would go to the identity operator, $\mathcal{S}_{l'm'lm} \to \delta_{ll'}\delta_{mm'}$, and $\phi_{lm}(\mathbf{x})$ would reduce to $2j_l(kr)Y_{lm}(\hat{\mathbf{x}})$, the partial wave solution regular at the origin. It is convenient to make this result explicit by rewriting Eq. (2.17) as

$$\phi_{lm}(\mathbf{x}) = 2j_l(kr)Y_{lm}(\hat{\mathbf{x}}) + \sum_{l'm'} 2\mathcal{T}_{l'm'lm}(k)h_{l'}^{(1)}(kr)Y_{l'm'}(\hat{\mathbf{x}}), \tag{2.19}$$

where $\mathcal{T}$ is the *transition matrix* or $\mathbb{T}$-matrix[4]

$$\mathcal{T}_{l'm'lm}(k) \equiv \langle l'm'|\mathbb{T}(k)|lm\rangle = \tfrac{1}{2}(\mathcal{S}_{l'm'lm}(k) - \delta_{l'l}\delta_{m'm}). \tag{2.20}$$

Unitarity requires $\mathbb{S}^\dagger\mathbb{S} = \mathbb{I}$, or $\sum_{l'm'}\mathcal{S}^*_{l'm'l''m''}\mathcal{S}_{l'm'lm} = \delta_{l''l}\delta_{m''m}$. Time reversal symmetry requires that $\mathcal{S}_{l'm'lm}$ is symmetric in $(l, m) \leftrightarrow (l', m')$. If the object Σ is spherically symmetric, $\mathbb{S}$ and $\mathbb{T}$ are diagonal in ℓ and m. However we are also interested in more general cases where the material objects do not have any special symmetry.

It is useful to review the connection between $\mathcal{T}_{l'm'lm}(k)$ and the scattering of ϕ from the object. The scattering amplitude is defined as the response of the object to an incoming plane wave. Since angular momentum is not conserved, we have to keep track of the direction of the incoming plane wave. The solution to the Helmholtz equation that reduces at $r \to \infty$ to a plane wave with wave vector $\mathbf{k}$ accompanied by an outgoing scattered wave defines the scattering amplitude, $f(\mathbf{k}, \mathbf{k}')$,

$$\begin{aligned}\Phi(\mathbf{k}, \mathbf{x}) &= 2\pi\sum_{lm}\phi_{lm}(\mathbf{x})i^l Y^*_{lm}(\hat{\mathbf{k}}) \\ &\sim e^{i\mathbf{k}\cdot\mathbf{x}} + \frac{e^{ikr}}{r}f(\mathbf{k}, \mathbf{k}') \quad \text{as } r \to \infty,\end{aligned} \tag{2.21}$$

where $\mathbf{k}' \equiv k\hat{\mathbf{x}}$ is the wave vector of the observed wave. The differential cross section is given by

$$\frac{d\sigma}{d\Omega} = |f(\mathbf{k}, \mathbf{k}')|^2. \tag{2.22}$$

To relate $f(\mathbf{k}, \mathbf{k}')$ to $\mathbb{T}$ we express the plane wave as a superposition of partial waves,

$$e^{i\mathbf{k}\cdot\mathbf{x}} = 4\pi\sum_{lm} j_l(kr)i^l Y_{lm}(\hat{\mathbf{x}})Y^*_{lm}(\hat{\mathbf{k}}), \tag{2.23}$$

where the unit vectors $\hat{\mathbf{x}}$ and $\hat{\mathbf{k}}$ specify the polar angles of $\mathbf{x}$ and $\mathbf{k}$ with respect to an arbitrary axis. We identify what remains with the scattered wave,

$$\Phi(\mathbf{k}, \mathbf{x}) = e^{i\mathbf{k}\cdot\mathbf{x}} + 4\pi\sum_{l'm'lm} i^l\mathcal{T}_{l'm'lm}(k)h_{l'}^{(1)}(kr) \times Y_{l'm'}(\hat{\mathbf{x}})Y^*_{lm}(\hat{\mathbf{k}}). \tag{2.24}$$

Using the asymptotic form of the Hankel functions, $h_l^{(1)}(kr) \to i^{-l-1}e^{ikr}/kr$, we obtain

$$f(\mathbf{k}, \mathbf{k}') = \frac{4\pi}{ik}\sum_{l'm'lm} i^{l-l'}\mathcal{T}_{l'm'lm}(k)Y_{l'm'}(\hat{\mathbf{k}}')Y^*_{lm}(\hat{\mathbf{k}}). \tag{2.25}$$

When angular momentum is conserved, $\mathcal{S}_{l'm'lm}(k) = e^{2i\delta_l(k)}\delta_{ll'}\delta_{mm'}$ and we obtain the standard result $f(\mathbf{k}, \mathbf{k}') = \sum_l(2l+1)f_l(k)P_l(\cos\theta_{\hat{\mathbf{k}}\hat{\mathbf{k}}'})$, with $f_l(k) = \frac{1}{k}\sin\delta_l(k)e^{i\delta_l(k)}$.

Finally, we will need the partial wave expansion for the *free*, outgoing wave Helmholtz Green's function,

$$\begin{aligned}\mathcal{G}_0(\mathbf{x}, \mathbf{x}', k) &\equiv \frac{e^{ik|\mathbf{x}-\mathbf{x}'|}}{4\pi|\mathbf{x}-\mathbf{x}'|} \\ &= ik\sum_{lm} j_l(kr_<)h_l^{(1)}(kr_>)Y_{lm}(\hat{\mathbf{x}})Y^*_{lm}(\hat{\mathbf{x}}') \\ &= ik\sum_{lm} j_l(kr_<)h_l^{(1)}(kr_>)Y_{lm}(\hat{\mathbf{x}}')Y^*_{lm}(\hat{\mathbf{x}}),\end{aligned} \tag{2.26}$$

where the notations $r_{<(>)}$ refer to whichever of r, r' is the smaller (larger).

C. Low energy scattering and the coefficients of capacitance

As $k \to 0$, the Helmholtz equation reduces to Laplace's equation. Therefore we can relate the low energy limit of the $\mathbb{S}$-matrix elements to the parameters that describe solutions to Laplace's equation, which are tensor generalizations of capacitance. In this subsection we continue to suppress the label α that distinguishes the particular object of interest.

At large distances, solutions to Laplace's equation are of the form $r^l Y_{lm}(\hat{\mathbf{x}})$ or $r^{-l-1}Y_{lm}(\hat{\mathbf{x}})$. If an object is placed in an external field (potential) of the first form, then its response, determined by the boundary condition $\phi = 0$ on the surface, is of the second form. The monopole response to an asymptotically constant field defines the capacitance; the dipole response to an asymptotically dipole field defines the polarizability, and so forth. Therefore we parameterize a solution to Laplace's equation that goes to $r^l Y_{lm}(\hat{\mathbf{x}})$ by[5]

$$\phi_{lm}(\mathbf{x}) \propto r^l Y_{lm}(\hat{\mathbf{x}}) - \sum_{l'm'}\mathcal{C}_{l'm'lm}\frac{Y_{l'm'}(\hat{\mathbf{x}})}{r^{l'+1}}. \tag{2.27}$$

For a Dirichlet boundary condition the $\{C_{l'm'lm}\}$ are the tensor generalizations of the capacitance. For other bound-

[4]Our definition of the $\mathbb{T}$-matrix differs by a factor i from some conventional choices [36].

[5]Note the minus sign that preserves the usual definition of capacitance. When an object is held at a voltage V, its charge is $Q = CV$. Equivalently, when the object is grounded and the potential at infinity is V, the induced monopole field is $-CV/r$.

ary conditions, the physical connection to electrostatics is lost, but the tensor structure (and the connection to the $\mathcal{S}$-matrix) remains.

Taking the limit $k \to 0$ in Eq. (2.19) we obtain an expression for ϕ_{lm} in terms of the $k \to 0$ limit of the T-matrix,

$$\lim_{k\to 0}\phi_{lm}(\mathbf{x}) \sim \frac{2(kr)^l}{(2l+1)!!}Y_{lm}(\hat{\mathbf{x}}) - 2i\sum_{l'm'}\mathcal{T}_{l'm'lm}(k) \times \frac{(2l'-1)!!}{(kr)^{(l'+1)}}Y_{l'm'}(\hat{\mathbf{x}}). \tag{2.28}$$

In order to obtain a finite and nonvanishing limit, we find $\mathcal{T}_{l'm'lm}(k) \sim k^{l+l'+1}$ as $k \to 0$, a standard result. Comparing these two expressions we find

$$\lim_{k\to 0}\frac{1}{k^{l+l'+1}}\mathcal{T}_{l'm'lm}(k) = \frac{-iC_{l'm'lm}}{(2l+1)!!(2l'-1)!!}. \tag{2.29}$$

Some special cases deserve mention. For $l = l' = 0$, as $k \to 0$, $\mathcal{T}_{0000}(k) \sim -ika$, where a is the scattering length. Comparing Eqs. (2.28) and (2.29) we see that the capacitance, $C \equiv C_{0000}$, equals the scattering length. The $l = 0$, $l' = 1$ coefficient describes the dipole moment developed by a conductor in response to a constant external potential (or, by symmetry, the charge induced by an external dipole field). It vanishes for spherically symmetric objects, but more generally we can choose the origin of the coordinate system so that $C_{1m00} = C_{001m} = 0$. From now on we assume that the origin, $\mathcal{O}_\alpha$, within the object Σ_α has been chosen to eliminate this dipole response. The $l = l' = 1$ coefficients describe the dipole response to an external dipole field: these nine components form the tensor (electrostatic) polarizability.

Finally, we note that the coefficients $C_{l'm'lm}$ can be interpreted as the components of an abstract tensor $\mathbb{C}_{l'l}$ in a spherical basis. $\mathbb{C}_{l'l}$ is the exterior product of two irreducible tensors, one rank l and the other rank l'. It is sometimes useful to project $\mathbb{C}_{l'l}$ into its irreducible components. Thus, for example, $\mathbb{C}_{11}$, the electrostatic polarizability, can be decomposed into its trace, the scalar polarizability, and a traceless part that describes the aspherical response of the object.

D. Translation formulas

Partial wave solutions to the Helmholtz equation for an object Σ_α, defined with respect to the origin $\mathcal{O}_\alpha$, can be expanded in partial waves with respect to a second origin $\mathcal{O}_\beta$ within a second object Σ_β. The objects, coordinate origins, and notation for vectors are shown in Fig. 1. Any solution with definite angular momentum defined with respect to $\mathcal{O}_\alpha$, whether regular (j_l) or outgoing ($h_l^{(1)}$), is regular when viewed from $\mathcal{O}_\beta$. Therefore it is possible to

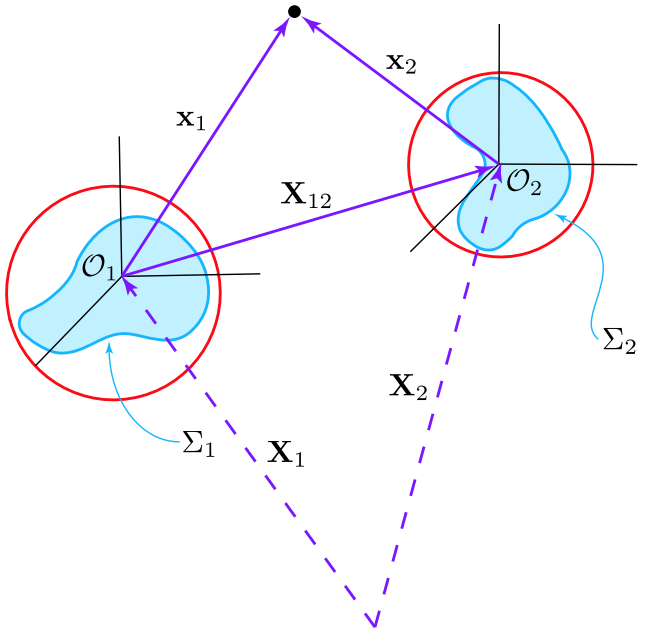

FIG. 1 (color online). Two objects enclosed by the surfaces Σ_1 and Σ_2 are shown, each with bounding spheres (radii R_1 and R_2). We assume that it is possible to choose bounding spheres that do not overlap. Coordinate systems with parallel axes are erected at origins $\mathcal{O}_1$ and $\mathcal{O}_2$ at positions $\mathbf{X}_1$ and $\mathbf{X}_2$. The origins are chosen so that the dipole coefficients of capacitance, C_{001m}, vanish. Coordinate vectors $\mathbf{x}_1$ and $\mathbf{x}_2$ to an arbitrary point, $\mathbf{x}$, are shown. The vector from $\mathcal{O}_1$ to $\mathcal{O}_2$ is $\mathbf{X}_{12} = \mathbf{X}_2 - \mathbf{X}_1 = \mathbf{x}_1 - \mathbf{x}_2$. The distance between the two objects is $d_{12} = |\mathbf{X}_{12}|$.

expand both in terms of spherical Bessel functions $j_l(kr_\beta)$ with respect to $\mathcal{O}_\beta$,

$$\begin{aligned} j_l(kr_\alpha)Y_{lm}(\hat{\mathbf{x}}_\alpha) &= \sum_{l'm'}\mathcal{V}^{\beta\alpha}_{l'm'lm}(\mathbf{X}_{\beta\alpha})j_{l'}(kr_\beta)Y_{l'm'}(\hat{\mathbf{x}}_\beta) \\ h_l^{(1)}(kr_\alpha)Y_{lm}(\hat{\mathbf{x}}_\alpha) &= \sum_{l'm'}\mathcal{U}^{\beta\alpha}_{l'm'lm}(\mathbf{X}_{\beta\alpha})j_{l'}(kr_\beta)Y_{l'm'}(\hat{\mathbf{x}}_\beta) \end{aligned} \tag{2.30}$$

for $r_\beta < d_{\alpha\beta}$. Note that $\mathbf{x}_\alpha$ and $\mathbf{x}_\beta$ refer to the coordinate components of a point $\mathbf{x}$ relative to the origin $\mathcal{O}_\alpha$ or $\mathcal{O}_\beta$ respectively. The matrices $\mathbb{U}$ and $\mathbb{V}$ that define the change of basis depend on the vector from $\mathcal{O}_\alpha$ to $\mathcal{O}_\beta$, $\mathbf{X}_{\alpha\beta} = \mathbf{X}_\beta - \mathbf{X}_\alpha = \mathbf{x}_\alpha - \mathbf{x}_\beta$, as defined in Fig. 1. These formulas are known in the literature as translation formulas. A brief derivation of the translation formulas can be found in Appendix C and further discussion in Ref. [20].

Without loss of generality, to simplify the formulas we take the Cartesian unit vectors that define the orientations of the reference frames all to be parallel. We will need only formulas that apply to the outgoing solutions,

$$\mathcal{U}^{\alpha\beta}_{l'm'lm}(\mathbf{X}_{\alpha\beta}) = \sqrt{4\pi}(-1)^{m'} i^{l-l'}\sqrt{(2l+1)(2l'+1)} \times \sum_{l''m''} (-1)^{m''} i^{l''}\sqrt{2l''+1}\begin{pmatrix} l & l' & l'' \\ 0 & 0 & 0 \end{pmatrix} \times \begin{pmatrix} l & l' & l'' \\ m & -m' & -m'' \end{pmatrix} h^{(1)}_{l''}(kd_{\alpha\beta}) \times Y_{l''m''}(\hat{\mathbf{X}}_{\alpha\beta}). \quad (2.31)$$

The summation over l'' involves only a finite number of terms since the 3-j symbols vanish for $l'' > l + l'$ and $l'' < |l - l'|$. Moreover they are zero if $l + l' + l''$ is odd or if $m'' \neq m - m'$. The matrix $\mathcal{U}^{\alpha\beta}_{l'm'lm}$ has the following symmetries,

$$\mathcal{U}^{\alpha\beta}_{l'm'lm} = (-1)^{l+l'} e^{2i(m-m')\phi_{\alpha\beta}} \mathcal{U}^{\alpha\beta}_{lml'm'}, \quad (2.32)$$

$$\mathcal{U}^{\alpha\beta}_{l'm'lm} = (-1)^{m+m'} e^{2i(m-m')\phi_{\alpha\beta}} \mathcal{U}^{\alpha\beta}_{l'-m'l-m}, \quad (2.33)$$

$$\mathcal{U}^{\beta\alpha}_{l'm'lm} = (-1)^{l+l'} \mathcal{U}^{\alpha\beta}_{l'm'lm}, \quad (2.34)$$

where $\phi_{\alpha\beta}$ is the azimuthal angle of the translation. If we are considering only two objects, then it is always possible to orient the Cartesian coordinate systems so that they are related by translation along the z-axis. In this case $\mathcal{U}^{\alpha\beta}_{l'm'lm}$ simplifies. For $\mathbf{X}_{\alpha\beta} = \pm d_{\alpha\beta}\hat{\mathbf{z}}$ one obtains, using $Y_{l''m''}(\pm\hat{\mathbf{z}}) = (\pm)^{l''}\sqrt{(2l''+1)/4\pi}\delta_{m''0}$,

$$\mathcal{U}^{\alpha\beta}_{l'm'lm}(\pm d_{\alpha\beta}\hat{\mathbf{z}}) = \delta_{m'm}(-1)^m i^{l-l'}\sqrt{(2l+1)(2l'+1)} \times \sum_{l''} i^{\pm l''}(2l''+1)\begin{pmatrix} l & l' & l'' \\ 0 & 0 & 0 \end{pmatrix} \times \begin{pmatrix} l & l' & l'' \\ m & -m & 0 \end{pmatrix} h^{(1)}_{l''}(kd_{\alpha\beta}). \quad (2.35)$$

III. EVALUATION OF THE CASIMIR ENERGY

A. Performing the integral over ϕ

We start with the expression for the fixed-k functional integral, Eq. (2.13). For any fixed sources, $\{\varrho_\alpha\}$, there is a unique classical field, $\phi_{\rm cl}[\varrho]$, that is the solution to $\delta\tilde{S}[\phi, \varrho]/\delta\phi(\mathbf{x}) = 0$. The classical theory defined by $\tilde{S}[\phi, \varrho]$, describes a complex scalar field coupled to a set of sources on the surfaces, and is a generalization of electrostatics. By analogy with electrostatics, the field ϕ is continuous throughout space, but its normal derivative jumps by $\varrho_\alpha(\mathbf{x})$ across Σ_a. Indeed, the classical equations of motion that follow from $\delta\tilde{S}/\delta\phi = 0$ are

$$\begin{aligned} (\nabla^2 + k^2)\phi_{\rm cl}(\mathbf{x}) &= 0, \quad \text{for } \mathbf{x} \notin \Sigma_\alpha, \\ \Delta\phi_{\rm cl}(\mathbf{x}) &= 0, \quad \text{for } \mathbf{x} \in \Sigma_\alpha, \\ \Delta\partial_n\phi_{\rm cl}|_{\mathbf{x}} &= \varrho_\alpha(\mathbf{x}), \quad \text{for } \mathbf{x} \in \Sigma_\alpha, \end{aligned} \quad (3.1)$$

where $\Delta\phi = \phi_{\rm in} - \phi_{\rm out}$ and $\Delta\partial_n\phi = \partial_n\phi|_{\rm in} - \partial_n\phi_{\rm out}$. The subscripts "in" and "out" refer to the field inside and outside the bounding surface Σ_α. As before, all normals point out of the compact surfaces. The solution to Eq. (3.1) is unique up to solutions of the homogeneous equations, which we exclude by demanding that $\phi_{\rm cl}$ vanish when the $\{\varrho_\alpha\} = 0$. Continuing the analogy with electrostatics, we can write the classical field in terms of the free Green's function and the sources,

$$\phi_{\rm cl}(\mathbf{x}) = \sum_\beta \int_{\Sigma_\beta} d\mathbf{x}' \mathcal{G}_0(\mathbf{x}, \mathbf{x}', k)\varrho_\beta(\mathbf{x}'), \quad (3.2)$$

where $\mathcal{G}_0$ is the free Green's function given in Eq. (2.26).

To compute the functional integral over ϕ, we first decompose ϕ into the classical part given by Eq. (3.2) and a fluctuating part,

$$\phi(\mathbf{x}) = \phi_{\rm cl}(\mathbf{x}) + \delta\phi(\mathbf{x}). \quad (3.3)$$

Then, because the effective action, $\tilde{S}$, is quadratic in ϕ, the $\delta\phi$ dependent terms are independent of $\phi_{\rm cl}$,

$$\mathcal{Z}_{\mathcal{C}}(k) = \prod_{\alpha=1}^{N} \int [\mathcal{D}\varrho_\alpha(\mathbf{x})] e^{i(T/\hbar)\tilde{S}_{\rm cl}[\varrho]} \int [\mathcal{D}\delta\phi(\mathbf{x})] \times \exp\left[i\frac{T}{\hbar} \int d\mathbf{x}(k^2|\delta\phi(\mathbf{x})|^2 - |\nabla\delta\phi(\mathbf{x})|^2) \right]. \quad (3.4)$$

The classical action can be simplified by using the equations of motion, Eq. (3.1), which make it possible to express the action entirely in terms of integrals over the surfaces $\{\Sigma_\alpha\}$,

$$\tilde{S}_{\rm cl}[\varrho] = \frac{1}{2}\sum_\alpha \int_{\Sigma_\alpha} d\mathbf{x}(\varrho^*_\alpha(\mathbf{x})\phi_{\rm cl}(\mathbf{x}) + \text{c.c.}), \quad (3.5)$$

where $\phi_{\rm cl}(\mathbf{x})$ is understood to be a functional of the sources ϱ_α.

The functional integral over $\delta\phi$ is *independent of the classical field* $\phi_{\rm cl}$ and defines the energy of the unconstrained vacuum fluctuations of ϕ. This term is divergent, or, more precisely, depends on some unspecified ultraviolet cutoff. However it can be discarded because it is independent of the sources and therefore common to $\mathcal{Z}_{\mathcal{C}}$ and $\mathcal{Z}_\infty$. Note that this result is an explicit demonstration of the contention of Ref. [37]: the Casimir force has nothing to do with the *vacuum* fluctuations of ϕ, but is instead a consequence of the interaction between fluctuating sources in the materials. It is therefore not directly relevant to the fluctuations that are conjectured to be associated with the dark energy.

From Eq. (3.2) it is clear that the solution to Eq. (3.1) obeys the superposition principle: $\phi_{\rm cl}(\mathbf{x})$ is a sum of contributions from each of the sources,

$$\phi_{\rm cl}(\mathbf{x}) = \sum_\beta \phi_\beta(\mathbf{x}), \quad (3.6)$$

where ϕ_β satisfies Eq. (3.1) with all sources set equal to zero except for ϱ_β. So the action can be expressed as a double sum over surfaces and over contributions to $\phi_{\rm cl}$ generated by different objects. This leaves a partition function, $\mathcal{Z}_{\mathcal{C}}(k)$, of the form

$$\mathcal{Z}_{\mathcal{C}}(k) = \prod_{\alpha=1}^{N} \int [\mathcal{D}\varrho_\alpha(\mathbf{x})] \times \exp\left[\frac{i}{2}\frac{T}{\hbar}\sum_{\alpha,\beta}\int_{\Sigma_\alpha} d\mathbf{x}(\varrho^*_\alpha(\mathbf{x})\phi_\beta(\mathbf{x}) + \text{c.c.})\right], \tag{3.7}$$

to be evaluated.

B. Evaluation of the classical action

The classical action in Eq. (3.7) contains two qualitatively different terms, the interaction between different sources, $\alpha \neq \beta$, and the self-interaction of the source ϱ_α. Both can be expressed as functions of the multipole moments of the sources on the surfaces.

1. Interaction terms: $\alpha \neq \beta$

Consider the contribution to the action from the field, ϕ_β, generated by the source, ϱ_β, integrated over the surface Σ_α,

$$\tilde{S}_{\beta\alpha} = \frac{1}{2}\int_{\Sigma_\alpha} d\mathbf{x}_\alpha(\varrho^*_\alpha(\mathbf{x}_\alpha)\phi_\beta(\mathbf{x}_\alpha) + \text{c.c.}), \tag{3.8}$$

where the subscript α on $\mathbf{x}_\alpha$ indicates that the integration runs over coordinates measured relative to the origin of object α. The field $\phi_\beta(\mathbf{x}_\beta)$, *measured relative to the origin of object* β, can be represented as an integral over its sources on the surface Σ_β as in Eq. (3.2). Since every point on Σ_α is outside of a sphere enclosing Σ_β, the partial wave representation of $\mathcal{G}_0$ simplifies. The coordinate $\mathbf{x}_>$ is always associated with $\mathbf{x}_\beta$ and $\mathbf{x}_<$ is identified with $\mathbf{x}'_\beta$, so Eq. (3.2) can be written

$$\phi_\beta(\mathbf{x}_\beta) = ik\sum_{lm} h^{(1)}_l(kr_\beta)Y_{lm}(\hat{\mathbf{x}}_\beta) \times \int_{\Sigma_\beta} d\mathbf{x}'_\beta j_l(kr'_\beta)Y^*_{lm}(\hat{\mathbf{x}}'_\beta)\varrho_\beta(\mathbf{x}'_\beta). \tag{3.9}$$

Note that the arguments of the Bessel functions and spherical harmonics are all defined relative to the origin $\mathcal{O}_\beta$. In particular, r'_β and $\hat{\mathbf{x}}'_\beta$ are the radial and angular coordinates relative to $\mathcal{O}_\beta$ corresponding to a point $\mathbf{x}'$ on the surface Σ_β. The integrals over Σ_β define the *multipole moments* of the source ϱ_β, which will be our final quantum variables,

$$Q_{\beta,lm} \equiv \int_{\Sigma_\beta} d\mathbf{x}_\beta j_l(kr_\beta)Y^*_{lm}(\hat{\mathbf{x}}_\beta)\varrho_\beta(\mathbf{x}_\beta), \tag{3.10}$$

so that

$$\phi_\beta(\mathbf{x}_\beta) = ik\sum_{lm} Q_{\beta,lm}h^{(1)}_l(kr_\beta)Y_{lm}(\hat{\mathbf{x}}_\beta). \tag{3.11}$$

The field ϕ_β viewed from the surface Σ_α is a superposition of solutions to the Helmholtz equation that are regular at the origin $\mathcal{O}_\alpha$. Using the translation formulas, Eq. (2.30), the field generated by object Σ_β can be written as function of the coordinate $\mathbf{x}_\alpha$, measured from the origin $\mathcal{O}_\alpha$, as

$$\phi_\beta(\mathbf{x}_\alpha) = ik\sum_{lm} Q_{\beta,lm}\sum_{l'm'} \mathcal{U}^{\alpha\beta}_{l'm'lm} j_{l'}(kr_\alpha)Y_{l'm'}(\hat{\mathbf{x}}_\alpha). \tag{3.12}$$

This result, in turn, can be substituted into the contribution $\tilde{S}_{\beta\alpha}$ to the action, leading to the simple result

$$\tilde{S}_{\beta\alpha}[Q_\alpha, Q_\beta] = \frac{ik}{2}\sum_{lml'm'} Q^*_{\alpha,l'm'}\mathcal{U}^{\alpha\beta}_{l'm'lm}Q_{\beta,lm} + \text{c.c.} \tag{3.13}$$

Note that the contributions to the action that couple fields and sources on different objects make no reference to the particular boundary conditions that characterize the Casimir problem. They depend only on the multipole moments of the fields and on the geometry through the translation matrix $\mathbb{U}^{\alpha\beta}$.

2. Self-interaction terms

We turn to the terms in $\tilde{S}_{\rm cl}$ where the field and the source both refer to the same surface, Σ_α:

$$\tilde{S}_\alpha[\varrho_\alpha] = \frac{1}{2}\int_{\Sigma_\alpha} d\mathbf{x}(\varrho^*_\alpha(\mathbf{x})\phi_\alpha(\mathbf{x}) + \text{c.c.}). \tag{3.14}$$

For the self-interactions terms, we only use the coordinate system with origin $\mathcal{O}_\alpha$ inside the surface Σ_α, and hence drop the label α on the coordinates in this section. Since $\phi_\alpha(\mathbf{x})$ is continuous across the surface, we can regard the ϕ_α in Eq. (3.14) as the field *inside* Σ_α, $\phi_{{\rm in},\alpha}$, which is a solution to Helmholtz's equation that must be regular at the origin $\mathcal{O}_\alpha$,

$$\phi_{{\rm in},\alpha}(\mathbf{x}) = \sum_{lm}\phi_{\alpha,lm}j_l(kr)Y_{lm}(\hat{\mathbf{x}}). \tag{3.15}$$

Substituting this expansion into Eq. (3.14), we obtain

$$\tilde{S}_\alpha[\varrho_\alpha] = \frac{1}{2}\sum_{lm}(\phi_{\alpha,lm}Q^*_{\alpha,lm} + \text{c.c.}), \tag{3.16}$$

where the $Q_{\alpha,lm}$ are the multipole moments of the sources, defined in the previous subsection.

Finally we relate $\phi_{\alpha,lm}$ back to the multipole moments of the source to get an action entirely in terms of the $Q_{\alpha,lm}$. The field $\phi_{\alpha,{\rm out}}$ at points *outside* of Σ_α obeys Helmholtz's equation and must equal $\phi_{\alpha,{\rm in}}$ on the surface S. Therefore it can be written as $\phi_{\alpha,{\rm in}}$ *plus a superposition of the regular solutions to the Helmholtz equation that vanish on* Σ_α, as defined in Eq. (2.19),

$$\phi_{\alpha,\mathrm{out}}(\mathbf{x}) = \phi_{\alpha,\mathrm{in}}(\mathbf{x}) + \Delta\phi_\alpha(\mathbf{x}) = \phi_{\alpha,\mathrm{in}}(\mathbf{x}) + \sum_{lm}\chi_{\alpha,lm}\Big(j_l(kr)Y_{lm}(\hat{\mathbf{x}}) + \sum_{l'm'}\mathcal{T}^{\alpha}_{l'm'lm}(k)h^{(1)}_{l'}(kr)Y_{l'm'}(\hat{\mathbf{x}})\Big). \quad (3.17)$$

The second term, $\Delta\phi_\alpha$, vanishes on Σ_α because $\mathbb{T}^\alpha$ is the scattering amplitude for the Dirichlet problem.

The field we seek is generated in response to the sources and therefore falls exponentially (for k with positive imaginary part) as $r \to \infty$. Therefore the terms in Eq. (3.17) that are proportional to $j_l(kr)$ must cancel. Comparing Eq. (3.17) with Eq. (3.15), we conclude that $\chi_{\alpha,lm} = -\phi_{\alpha,lm}$, and therefore

$$\phi_{\alpha,\mathrm{out}}(\mathbf{x}) = -\sum_{lm}\phi_{\alpha,lm}\sum_{l'm'}\mathcal{T}^{\alpha}_{l'm'lm}(k)h^{(1)}_{l'}(kr)Y_{l'm'}(\hat{\mathbf{x}}). \quad (3.18)$$

On the other hand, $\phi_{\alpha,\mathrm{out}}(\mathbf{x})$ can be expressed as an integral over the source as in Eq. (3.2),

$$\phi_{\alpha,\mathrm{out}}(\mathbf{x}) = \int_{\Sigma_\alpha} d\mathbf{x}'\,\mathcal{G}_0(\mathbf{x},\mathbf{x}',k)\varrho_\alpha(\mathbf{x}'). \quad (3.19)$$

Using the partial wave expansion for the free Green's function, Eq. (2.26), we find

$$\phi_{\alpha,\mathrm{out}}(\mathbf{x}) = ik\sum_{l'm'}Q_{\alpha,l'm'}h^{(1)}_{l'}(kr)Y_{l'm'}(\hat{\mathbf{x}}), \quad (3.20)$$

and comparing with Eq. (3.18), we see that

$$ikQ_{\alpha,l'm'} = -\sum_{lm}\mathcal{T}^{\alpha}_{l'm'lm}(k)\phi_{\alpha,lm},$$

or

$$\phi_{\alpha,lm} = -ik\sum_{l'm'}[\mathcal{T}^{\alpha}]^{-1}_{lml'm'}Q_{\alpha,l'm'}, \quad (3.21)$$

where $[\mathbb{T}^\alpha]^{-1}$ is the inverse of the Dirichlet transition matrix $\mathbb{T}^\alpha$. When this is combined with Eq. (3.16), we obtain the desired expression for the self-interaction contribution to the action,

$$\tilde{S}_\alpha[Q_\alpha] = -\frac{ik}{2}\sum_{lml'm'}Q^*_{\alpha,lm}[\mathcal{T}^{\alpha}]^{-1}_{lml'm'}Q_{\alpha,l'm'} + \mathrm{c.c.}. \quad (3.22)$$

C. Evaluation of the integral over sources

Combining Eq. (3.22) with Eq. (3.13), we obtain an expression for the action that is a quadratic functional of the multipole moments of the sources on the surfaces. The functional integral Eq. (3.7) can be evaluated by changing variables from the sources, $\{\varrho_\alpha\}$ to the multipole moments. The functional determinant that results from this change of variables can be discarded because it is a common factor which cancels between $\mathfrak{Z}_\mathcal{C}$ and $\mathfrak{Z}_\infty$. To compute the functional integral we analytically continue to imaginary frequency, $k = i\kappa$, $\kappa > 0$,

$$\mathfrak{Z}_\mathcal{C}(i\kappa) = \prod_{\alpha=1}^{N}\int[\mathcal{D}Q_\alpha\mathcal{D}Q^*_\alpha]\exp\Big\{-\frac{\kappa}{2}\frac{T}{\hbar}\times\sum_\alpha Q^*_\alpha[\mathbb{T}^\alpha]^{-1}Q_\alpha + \frac{\kappa}{2}\frac{T}{\hbar}\sum_{\alpha\neq\beta}Q^*_\alpha\mathbb{U}^{\alpha\beta}Q_\beta + \mathrm{c.c.}\Big\}, \quad (3.23)$$

where we have suppressed the partial wave indices. The functional integral equation (3.23) yields the inverse determinant of a matrix $\mathbb{M}^{\alpha\beta}_\mathcal{C}$ that is composed of the inverse transition matrices $[\mathbb{T}^\alpha]^{-1}$ on its diagonal and the translation matrices $\mathbb{U}^{\alpha\beta}$ on the off-diagonals:

$$\mathbb{M}^{\alpha\beta}_\mathcal{C} = [\mathbb{T}^\alpha]^{-1}\delta_{\alpha\beta} - \mathbb{U}^{\alpha\beta}(1-\delta_{\alpha\beta}). \quad (3.24)$$

Finally we substitute into Eq. (2.10) to obtain the Casimir energy,

$$\mathcal{E}[\mathcal{C}] = \frac{\hbar c}{\pi}\int_0^\infty d\kappa\,\ln\frac{\det\mathbb{M}_\mathcal{C}(i\kappa)}{\det\mathbb{M}_\infty(i\kappa)}, \quad (3.25)$$

where the determinant is taken with respect to the partial wave indices and the object indices α, β, and $\mathbb{M}^{\alpha\beta}_\infty = [\mathbb{T}^\alpha]^{-1}\delta_{\alpha\beta}$ is the result of removing the objects to infinite separation, where the interaction effects vanish.

In the special case of two interacting objects Eq. (3.25) simplifies to

$$\mathcal{E}_2[\mathcal{C}] = \frac{\hbar c}{\pi}\int_0^\infty d\kappa\,\ln\det(1-\mathbb{T}^1\mathbb{U}^{12}\mathbb{T}^2\mathbb{U}^{21}), \quad (3.26)$$

where $\mathbb{T}^\alpha$, $\alpha = 1, 2$, and $\mathbb{U}^{\alpha\beta}$ are the transition and translation matrices for the two objects.

For three objects $\mathcal{E}$ takes the form,

$$\mathcal{E}_3[\mathcal{C}] = \frac{\hbar c}{\pi}\int_0^\infty d\kappa\Big\{\ln\det(1-\mathbb{T}^2\mathbb{U}^{21}\mathbb{T}^1\mathbb{U}^{12}) + \ln\det(1-\mathbb{T}^3\mathbb{U}^{31}\mathbb{T}^1\mathbb{U}^{13}) + \ln\det[1-(1-\mathbb{T}^3\mathbb{U}^{31}\mathbb{T}^1\mathbb{U}^{13})^{-1}\times(\mathbb{T}^3\mathbb{U}^{32}+\mathbb{T}^3\mathbb{U}^{31}\mathbb{T}^1\mathbb{U}^{12})(1-\mathbb{T}^2\mathbb{U}^{21}\mathbb{T}^1\mathbb{U}^{12})^{-1}\times(\mathbb{T}^2\mathbb{U}^{23}+\mathbb{T}^2\mathbb{U}^{21}\mathbb{T}^1\mathbb{U}^{13})]\Big\}. \quad (3.27)$$

Although this result appears complicated, it admits a simple physical interpretation. The first two terms describe scatterings between objects 1 and 2 and objects 1 and 3, and hence correspond to the separate two-body Casimir energies of these two pairs of objects. The third term must have a more complicated form because fluctuation forces are not pairwise additive and hence the third term is *not* simply given by the two-body Casimir energy of objects 2 and 3. The interaction of objects 2 and 3 involves not only

direct scatterings between these two objects but also indirect multiple scatterings off object 1. The third term in Eq. (3.27) contains the resolvent of the operator $\mathbb{T}^3\mathbb{U}^{31}\mathbb{T}^1\mathbb{U}^{13}$, which can be formally expanded as the series $\sum_{n=0}^{\infty}(\mathbb{T}^3\mathbb{U}^{31}\mathbb{T}^1\mathbb{U}^{13})^n$. The resolvent of $\mathbb{T}^2\mathbb{U}^{21}\mathbb{T}^1\mathbb{U}^{12}$ can be treated similarly. These series describe multiple scatterings between objects 1 and 3, and objects 1 and 2, respectively, which occur as intermediate steps in the scattering processes between objects 2 and 3. Inserting the series into the last term of Eq. (3.27), one can distinguish four qualitatively different scattering processes, described by the following operators,

$$\begin{aligned}
\mathbb{O}_1(m,n) &= (\mathbb{T}^3\mathbb{U}^{31}\mathbb{T}^1\mathbb{U}^{13})^m\mathbb{T}^3\mathbb{U}^{32}(\mathbb{T}^2\mathbb{U}^{21}\mathbb{T}^1\mathbb{U}^{12})^n\mathbb{T}^2\mathbb{U}^{23}\\
\mathbb{O}_2(m,n) &= (\mathbb{T}^3\mathbb{U}^{31}\mathbb{T}^1\mathbb{U}^{13})^m\mathbb{T}^3\mathbb{U}^{32}(\mathbb{T}^2\mathbb{U}^{21}\mathbb{T}^1\mathbb{U}^{12})^n\\
&\quad\times\mathbb{T}^2\mathbb{U}^{21}\mathbb{T}^1\mathbb{U}^{13}\\
\mathbb{O}_3(m,n) &= (\mathbb{T}^3\mathbb{U}^{31}\mathbb{T}^1\mathbb{U}^{13})^m\mathbb{T}^3\mathbb{U}^{31}\mathbb{T}^1\mathbb{U}^{12}(\mathbb{T}^2\mathbb{U}^{21}\mathbb{T}^1\mathbb{U}^{12})^n\\
&\quad\times\mathbb{T}^2\mathbb{U}^{23}\\
\mathbb{O}_4(m,n) &= (\mathbb{T}^3\mathbb{U}^{31}\mathbb{T}^1\mathbb{U}^{13})^m\mathbb{T}^3\mathbb{U}^{31}\mathbb{T}^1\mathbb{U}^{12}(\mathbb{T}^2\mathbb{U}^{21}\mathbb{T}^1\mathbb{U}^{12})^n\\
&\quad\times\mathbb{T}^2\mathbb{U}^{21}\mathbb{T}^1\mathbb{U}^{13}. \qquad (3.28)
\end{aligned}$$

The operator $\mathbb{O}_1(0,0)=\mathbb{T}^3\mathbb{U}^{32}\mathbb{T}^2\mathbb{U}^{23}$ describes direct scatterings between objects 2 and 3 as if object 1 were absent, and hence yields the additive approximation for the energy. All additional operators of Eq. (3.28) describe the nonadditivity of the Casimir interaction between three objects. The corresponding scattering processes are depicted in Fig. 2. The operator $\mathbb{O}_1(m,n)$ describes two scatterings between objects 2 and 3 with m (n) scatterings between objects 3 (2) and 1 in between. The operators $\mathbb{O}_2(m,n)$ ($\mathbb{O}_3(m,n)$) correspond to a wave that travels from object 3 (2) to object 2 (3) and is reflected back to object 3 (2) from object 1 after multiple scatterings between objects 1 and 2, and 1 and 3, respectively. Finally, operator $\mathbb{O}_4(m,n)$ describes only indirect scattering processes between objects 2 and 3 that all go through object 1.

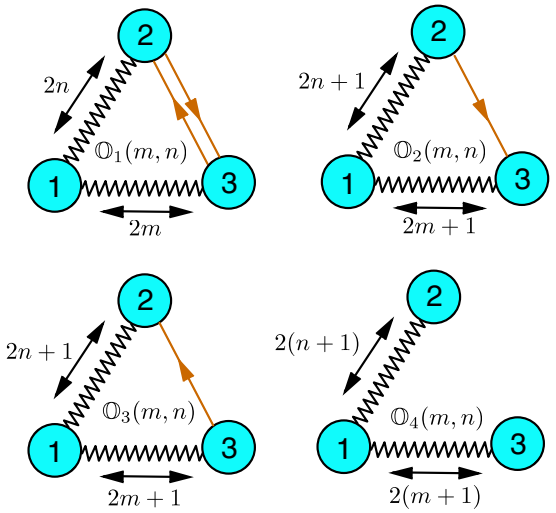

FIG. 2 (color online). Scattering processes described by the operators of Eq. (3.28). The directed lines between objects 2 and 3 describe a wave travelling once between the objects. The zigzag lines correspond to multiple reflections in both directions where the number next to the line indicates how many times the wave travels between the objects. To interpret the diagrams one starts with a wave at object 3. As an example, we describe explicitly the diagram for the operator $\mathbb{O}_1(m,n)$. The wave travels from object 3 to object 2, is then reflected $2n$ times back and forth between objects 2 and 1, travels back from object 2 to 3, and is finally reflected $2m$ times back and forth between objects 3 and 1. Each free propagation between the objects is described by the translation operator $\mathbb{U}^{\alpha\beta}$, and each reflection at an object by the transition operator $\mathbb{T}^{\alpha}$.

IV. APPLICATIONS

In this section we give a few typical applications of our method. Although the physically interesting case of electromagnetism requires vector fields and conducting boundary conditions, the scalar case offers an opportunity to check our methods and illustrate their utility. We consider a *real* scalar field fluctuating in the space between two spheres on which Robin boundary conditions, $\phi-\lambda_\alpha\partial_n\phi=0$, are imposed. Because a real field has half the oscillation modes of a complex field, the Casimir energy in Eq. (3.26) must be divided by 2, giving

$$\mathcal{E}_2[\mathcal{C}]=\frac{\hbar c}{2\pi}\int_0^\infty d\kappa\,\ln\det(1-\mathbb{T}^1\mathbb{U}^{12}\mathbb{T}^2\mathbb{U}^{21}). \qquad (4.1)$$

We allow for different Robin parameters $\lambda_{1,2}$ and different radii $R_{1,2}$ for the two spheres. This choice allows us to study Dirichlet ($\lambda/R\to 0$) and Neumann ($\lambda/R\to\infty$) boundary conditions on separate spheres as special cases. We obtain the Casimir energy as a series in R_1/d and R_2/d for large separations d and numerically at all separations. A comparison of the two approaches allows us to measure the rate of convergence of our results. We find that for Robin boundary conditions the sign of the force depends on the ratios λ_α/R_α and on the separation d. We also express the Casimir energy between two objects of general shape in a large distance expansion in terms of the coefficients of capacitance defined in Sec. II C.

A. Interaction of two spheres with Robin boundary conditions: general considerations

The Robin boundary condition $\phi-\lambda_\alpha\partial_n\phi=0$ allows a continuous interpolation between Dirichlet and Neumann boundary conditions. Since the radius of the sphere introduces a natural length scale, it is convenient to replace λ by a dimensionless variable, $\zeta_\alpha\equiv\lambda_\alpha/R_\alpha$. For $\zeta_\alpha>0$, the modulus of the field is suppressed if the surface is approached from the outside, while for $\zeta_\alpha<0$ it is enhanced. Hence, for negative ζ_α bound surface states can be expected. All the information about the shape of the object and the boundary conditions at its surface is provided by

the $\mathbb{T}$-matrix. For spherically symmetric objects the $\mathbb{T}$-matrix is diagonal and is completely specified by phase shifts $\delta_l(k)$ that do not depend on m,

$$\mathcal{T}_{lml'm'}(k) = \delta_{ll'}\delta_{mm'}\tfrac{1}{2}(e^{2i\delta_l(k)} - 1). \tag{4.2}$$

In the discussion of the $\mathbb{T}$-matrix for an individual object we again suppress the label α. The phase shifts for Robin boundary conditions are

$$\cot\delta_l(k) = \frac{n_l(\xi) - \zeta\xi n_l'(\xi)}{j_l(\xi) - \zeta\xi j_l'(\xi)}, \tag{4.3}$$

where $\xi = kR$ and $j_l(n_l)$ are spherical Bessel functions of first (second) kind. To apply Eq. (4.1), we have to evaluate the matrix elements of the transition matrices for imaginary frequencies $k = i\kappa$. Using $j_l(iz) = i^l\sqrt{\pi/(2z)}I_{l+1/2}(z)$ and $h_l^{(1)}(iz) = -i^{-l}\sqrt{2/(\pi z)}K_{l+1/2}(z)$, we obtain for the $\mathbb{T}$-matrix elements

$$\mathcal{T}_{lmlm}(i\kappa) = (-1)^l\frac{\pi}{2} \times \frac{(1/\zeta + 1/2)I_{l+1/2}(z) - zI_{l+1/2}'(z)}{(1/\zeta + 1/2)K_{l+1/2}(z) - zK_{l+1/2}'(z)}, \tag{4.4}$$

where $z \equiv \kappa R$.

For two spherical objects we can assume that the center-to-center distance vector is parallel to the z-axis. Then the translation matrices simplify to the form presented in Eq. (2.35). For imaginary frequencies the translation matrix elements become

$$\mathcal{U}^{\left\{\begin{smallmatrix}12\\21\end{smallmatrix}\right\}}_{l'mlm}(d) = -(-1)^m i^{-l'+l}\sqrt{(2l+1)(2l'+1)}\sum_{l''}(\pm 1)^{l''} \times (2l''+1)\begin{pmatrix} l & l' & l'' \\ 0 & 0 & 0\end{pmatrix}\begin{pmatrix} l & l' & l'' \\ m & -m & 0\end{pmatrix} \times\sqrt{\frac{2}{\pi\kappa d}}K_{l''+1/2}(\kappa d), \tag{4.5}$$

where d is the separation distance.

For a range of ζ, bound states can appear. This range can be determined by examining the $\mathbb{T}$-matrix at small frequencies, where it has the leading form

$$\mathcal{T}_{lmlm} \sim (-1)^l\frac{1 - l\zeta}{1 + (l+1)\zeta}z^{2l+1} + \ldots, \tag{4.6}$$

where we have suppressed positive numerical coefficients. The amplitudes diverge for $\zeta = \lambda/R = -1/(l+1)$ indicating the existence of a pole at $\kappa = 0$ at this value of ζ. Indeed, from Eq. (4.4) we find that the $\mathbb{T}$-matrix elements have a pole in the lth partial wave at $\kappa_l > 0$ if $-1/(l+1) < \zeta < 0$. The values of κ_l are determined by the equation

$$-\frac{1}{\zeta} = 1 + l + R\kappa_l\frac{K_{l-1/2}(R\kappa_l)}{K_{l+1/2}(R\kappa_l)}. \tag{4.7}$$

These poles correspond to bound states for $-1 < \zeta < 0$. For any ζ in this interval, there exists a finite number of bound states, which increases as $\zeta \to 0$. In the following, we restrict to $\zeta \geq 0$ and leave the study of interactions in the presence of bound states to a future publication.

The special case of spheres with Dirichlet boundary conditions has been studied in Ref. [28]. For two spheres of equal radius, the matrix $\sum_{l''}A^{(m)}_{ll''}A^{(m)}_{l''l'}$ in the notation of Ref. [28] is proportional to our $\mathbb{T}^1\mathbb{U}^{12}\mathbb{T}^2\mathbb{U}^{21}$ times $K_{l+1/2}(\kappa R)/K_{l'+1/2}(\kappa R)$. It is easy to see that this proportionality factor drops out in the final result for the energy if one uses ln det= tr ln in Eq. (4.1) and expands the logarithm around unity. Thus we agree with the results given in Ref. [28].

B. Asymptotic expansion for large separation

In this section we consider the Casimir interaction between two spheres due to a scalar field obeying Robin boundary conditions, allowing for a different parameter $\lambda_{1,2}$ on each sphere. The Casimir energy can be developed in an asymptotic expansion in R_α/d using ln det= tr ln in Eq. (4.1). Expanding the logarithm in powers of $\mathbb{N} = \mathbb{T}^1\mathbb{U}^{12}\mathbb{T}^2\mathbb{U}^{21}$, since the $\mathbb{T}$-matrix has no poles in the region of interest we get

$$\mathcal{E} = -\frac{\hbar c}{2\pi}\int_0^\infty d\kappa\sum_{p=1}^\infty\frac{1}{p}\,\mathrm{tr}(\mathbb{N}^p). \tag{4.8}$$

We have performed the matrix operations using MATHEMATICA. The scaling of the $\mathbb{T}$-matrix at small κ shows that the pth power of $\mathbb{N}$ (corresponding to $2p$ scatterings) becomes important at order $d^{-(2p+1)}$. Partial waves of order l start to contribute at order $d^{-(3+2l)}$ if the $\mathbb{T}$-matrix is diagonal in l, which is the case for spherically symmetric objects. Hence the leading terms with $p = 1$ and $l = 0$ yield the exact energy to order d^{-4}. In the following we will usually restrict the expansion to $p \leq 3$, $l \leq 2$, yielding the interaction to order d^{-8}.

1. Equal radii

We begin with the case $R_1 = R_2 = R$. The large distance expansion of the Casimir energy can be written as

$$\mathcal{E} = \frac{\hbar c}{\pi}\frac{1}{d}\sum_{j=3}^\infty b_j\left(\frac{R}{d}\right)^{j-1}, \tag{4.9}$$

where b_j is the coefficient of the term $\sim d^{-j}$. For general Robin boundary conditions we find

$$b_3 = -\frac{1}{4(1+\zeta_1)(1+\zeta_2)}, \tag{4.10}$$

$$b_4 = -\frac{(2+\zeta_1+\zeta_2)}{8(1+\zeta_1)^2(1+\zeta_2)^2}, \tag{4.11}$$

$$\begin{aligned} b_5 = {} & [-77 - 231(\zeta_1+\zeta_2) - (188(\zeta_1^2+\zeta_2^2) + 625\zeta_1\zeta_2) - 2(3(\zeta_1^3+\zeta_2^3) + 197(\zeta_1\zeta_2^2+\zeta_2\zeta_1^2)) + 2(17(\zeta_1^4+\zeta_2^4) \\ & + 56(\zeta_2\zeta_1^3+\zeta_1\zeta_2^3) - 18\zeta_1^2\zeta_2^2) + 2\zeta_1\zeta_2(68(\zeta_1^3+\zeta_2^3) + 155(\zeta_1\zeta_2^2+\zeta_2\zeta_1^2)) + 2\zeta_1^2\zeta_2^2(85(\zeta_1^2+\zeta_2^2) + 124\zeta_2\zeta_1) \\ & + 68\zeta_1^3\zeta_2^3(\zeta_1+\zeta_2)][48(1+\zeta_1)^3(1+2\zeta_1)(1+\zeta_2)^3(1+2\zeta_2)]^{-1}, \\ b_6 = {} & [-50 - 175(\zeta_1+\zeta_2) - (179(\zeta_1^2+\zeta_2^2) + 592\zeta_1\zeta_2) - (18(\zeta_1^3+\zeta_2^3) + 565(\zeta_1^2\zeta_2+\zeta_2^2\zeta_1)) + (64(\zeta_1^4+\zeta_2^4) \\ & + 6(\zeta_1^3\zeta_2+\zeta_1\zeta_2^3) - 460\zeta_1^2\zeta_2^2) + 2(11(\zeta_1^5+\zeta_2^5) + 136(\zeta_1^4\zeta_2+\zeta_1\zeta_2^4) + 67(\zeta_1^3\zeta_2^2+\zeta_1^2\zeta_2^3)) + 4\zeta_1\zeta_2(22(\zeta_1^4+\zeta_2^4) \\ & + 93(\zeta_1^3\zeta_2+\zeta_1\zeta_2^3) + 52\zeta_1^2\zeta_2^2) + 2\zeta_1^2\zeta_2^2(55(\zeta_1^3+\zeta_2^3) + 92(\zeta_1^2\zeta_2+\zeta_1\zeta_2^2)) + 4\zeta_1^3\zeta_2^3(11(\zeta_1^2+\zeta_2^2) + 8\zeta_1\zeta_2)] \\ & \times [32(1+\zeta_1)^4(1+2\zeta_1)(1+\zeta_2)^4(1+2\zeta_2)]^{-1}. \end{aligned} \tag{4.12}$$

Higher order coefficients can be obtained but are not shown here in order to save space. For special values of λ_α they are given below. These coefficients show some interesting properties. They all diverge for $\zeta_\alpha = -1$, where $\lambda_\alpha = -R_\alpha$, and b_5 and b_6 also diverge for $\zeta_\alpha = -1/2$. These results are consistent with the emergence of poles in the $\mathbb{T}$-matrix at small κ when ζ_α approaches $-1/(l+1)$ and the observation that the partial wave with $l = 1$ starts to contribute only at order d^{-5}. Another interesting property is that some coefficients b_j go to zero for $\lambda_\alpha \to \infty$, which corresponds to Neumann boundary conditions. If both λ_α go to infinity, the coefficients b_j vanish for $j = 1, \ldots, 6$, so that the leading term in the Casimir energy is $\sim d^{-7}$ with a negative amplitude. Hence, Neumann boundary conditions lead to an attractive Casimir-Polder power law, as is known from electromagnetic field fluctuations. This result can be understood from the absence of low-frequency s-waves for Neumann boundary conditions. It is clearly reflected by the low frequency expansion of Eq. (4.6), which has a vanishing amplitude for $\lambda_\alpha \to \infty$ if $l = 0$. If one λ_α remains finite and the other goes to infinity, only the coefficients b_3 and b_4 vanish so that the energy scales as d^{-5} with a *positive* amplitude. Since $b_3 < 0$ for $\lambda_\alpha \geq 0$, at asymptotic distances the Casimir force is therefore attractive for all non-negative finite λ_α, and for λ_α both infinite. It is repulsive if one λ_α is finite and the other infinite, i.e., if one sphere obeys Neumann boundary conditions. However, at smaller distances the interaction can change sign depending on λ_α, as shown below. Notice that the two spheres do not fall into the class of mirror symmetric configurations if the boundary conditions are different on the two spheres. Hence the conclusion of Ref. [32] does not apply to the cases where we obtain repulsion.

More precisely, one has the following limiting cases. If both $\lambda_\alpha = 0$, the field obeys Dirichlet conditions at the two spheres and the first six coefficients are

$$\begin{aligned} & b_3 = -\tfrac{1}{4}, \quad b_4 = -\tfrac{1}{4}, \quad b_5 = -\tfrac{77}{48}, \\ & b_6 = -\tfrac{25}{16}, \quad b_7 = -\tfrac{29\,837}{2880}, \quad b_8 = -\tfrac{6491}{1152}. \end{aligned} \tag{4.13}$$

If Neumann conditions are imposed on both surfaces, the coefficients are

$$\begin{aligned} & b_3 = 0, \quad b_4 = 0, \quad b_5 = 0, \quad b_6 = 0, \\ & b_7 = -\tfrac{161}{96}, \quad b_8 = 0, \quad b_9 = -\tfrac{3011}{192} \quad b_{10} = -\tfrac{175}{128}, \end{aligned} \tag{4.14}$$

clearly showing that the asymptotic interaction has a Casimir-Polder power law $\sim\mathcal{O}(d^{-7})$. Also, as in the electromagnetic case, the next to leading order $\mathcal{O}(d^{-8})$ vanishes [11]. Therefore we have included the two next terms of the series. If $\lambda_2 \to \infty$ (Neumann conditions) and λ_1 remains finite, we have

$$\begin{aligned} & b_3 = 0, \quad b_4 = 0, \quad b_5 = \frac{17}{48(1+\zeta_1)}, \\ & b_6 = \frac{11}{32(1+\zeta_1)^2}, \\ & b_7 = \frac{1989 + 4736\zeta_1 + 1895\zeta_1^2 - 2192\zeta_1^3 - 1610\zeta_1^4}{480(1+\zeta_1)^3(1+2\zeta_1)}, \\ & b_8 = \frac{5(94 + 143\zeta_1 + 76\zeta_1^2 - 45\zeta_1^3)}{288(1+\zeta_1)^4}. \end{aligned} \tag{4.15}$$

Thus, for mixed Dirichlet/Neumann boundary conditions, the result is

$$\begin{aligned} & b_3 = 0, \quad b_4 = 0, \quad b_5 = \frac{17}{48}, \\ & b_6 = \frac{11}{32}, \quad b_7 = \frac{663}{160}, \quad b_8 = \frac{235}{144}. \end{aligned} \tag{4.16}$$

Finally, if $\lambda_2 = 0$ (Dirichlet conditions) and λ_1 is finite, we obtain

$$\begin{aligned} & b_3 = -\frac{1}{4(1+\zeta_1)}, \quad b_4 = -\frac{(2+\zeta_1)}{8(1+\zeta_1)^2}, \\ & b_5 = -\frac{77 + 231\zeta_1 + 188\zeta_1^2 + 6\zeta_1^3 - 34\zeta_1^4}{48(1+\zeta_1)^3(1+2\zeta_1)}, \\ & b_6 = -\frac{50 + 175\zeta_1 + 179\zeta_1^2 + 18\zeta_1^3 - 64\zeta_1^4 - 22\zeta_1^5}{32(1+\zeta_1)^4(1+2\zeta_1)}, \end{aligned} \tag{4.17}$$

where we have not shown higher order coefficients. It is important to note that the series in Eq. (4.9) is an asymptotic series and therefore cannot be used to obtain the interaction at short distances.

2. Unequal radii

To study the individual contributions from two objects to the various terms in the large distance expansion, it is instructive to study two spheres of different radii R_1 and R_2. For simplicity, we focus on Dirichlet and Neumann boundary conditions. By expanding the energy in powers of $\mathbb{N}$ as before, we get an asymptotic expansion of the Casimir energy,

$$\mathcal{E} = \frac{\hbar c}{\pi}\frac{1}{d}\sum_{j=3}^{\infty}\tilde{b}_j(\eta)\left(\frac{R_1}{d}\right)^{j-1}, \tag{4.18}$$

where the coefficients now also depend on $\eta = R_2/R_1$. For Dirichlet boundary conditions on both spheres, the coefficients are

$$\begin{aligned}
\tilde{b}_3 &= -\frac{\eta}{4}, \quad \tilde{b}_4 = -\frac{\eta+\eta^2}{8}, \quad \tilde{b}_5 = -\frac{34(\eta+\eta^3)+9\eta^2}{48},\\
\tilde{b}_6 &= -\frac{2(\eta+\eta^4)+23(\eta^2+\eta^3)}{32},\\
\tilde{b}_7 &= -\frac{8352(\eta+\eta^5)+1995(\eta^2+\eta^4)+38980\eta^3}{5760},\\
\tilde{b}_8 &= -\frac{-1344(\eta+\eta^6)+5478(\eta^2+\eta^5)+2357(\eta^3+\eta^4)}{2304},
\end{aligned} \tag{4.19}$$

while for Neumann boundary conditions on both spheres, we have

$$\begin{aligned}
\tilde{b}_7 &= -\frac{161\eta^3}{96}, \qquad \tilde{b}_8 = 0,\\
\tilde{b}_9 &= -\frac{3011(\eta^3+\eta^5)}{384}, \qquad \tilde{b}_{10} = -\frac{175(\eta^3+\eta^6)}{256},
\end{aligned} \tag{4.20}$$

and for Dirichlet conditions on the sphere with radius R_1 and Neumann conditions on the one with radius R_2, we obtain

$$\begin{aligned}
\tilde{b}_5 &= \frac{17\eta^3}{48}, \qquad \tilde{b}_6 = \frac{11\eta^3}{32},\\
\tilde{b}_7 &= \frac{\eta^3(1610+379\eta^2)}{480},\\
\tilde{b}_8 &= \frac{5\eta^3(24+67\eta^2+3\eta^3)}{288}.
\end{aligned} \tag{4.21}$$

For like boundary conditions, the coefficients satisfy the symmetry condition $\eta^{j-1}\tilde{b}_j(1/\eta) = \tilde{b}_j(\eta)$. The coefficient $\tilde{b}_8$ for Dirichlet conditions becomes positive if η is sufficiently large or small compared to unity. Because of the absence of monopoles, Neumann conditions on one or both spheres lead to coefficients that scale at least as η^3. For the same reason, not all powers of η contribute to the coefficients if Neumann conditions are imposed. Note that the interaction between a sphere and a plate cannot be obtained from this asymptotic expansion as the limit $\eta \to 0$ since the expansion assumes that $R_1, R_2 \ll d$. However, the sphere-plate interaction can be computed by the same technique employed here if it is applied to the Green's function of the semi-infinite space bounded by the plate instead of the free Green's function.

C. Numerical results for Robin boundary conditions on two spheres at all separations

The primary application of our analysis is to compute the Casimir energy and force to high accuracy over a broad range of distances. However, to obtain the interaction at all distances, Eq. (4.1) has to be evaluated numerically. We shall see that the domain where our method is *least* accurate is when the two surfaces approach one another. That is the regime where semiclassical methods like the proximity force approximation (PFA) become exact. Because of its role in this limit, and because it is often used (with little justification) over wide ranges of separations, it is important to compare our calculations with the PFA predictions.

1. PFA for Robin boundary conditions

In the proximity force approximation, the energy is obtained as an integral over infinitesimal parallel surface elements at their local distance L, measured perpendicular to a surface Σ that can be one of the two surfaces of the objects, or an auxiliary surface placed between the objects. The PFA approximation for the energy is then given by

$$\mathcal{E}_{\mathrm{PFA}} = \frac{1}{A}\int_{\Sigma}\mathcal{E}_{\parallel}(L)dS, \tag{4.22}$$

where $\mathcal{E}_{\parallel}(L)/A$ is the energy per area for two parallel plates with distance L. Functional integral techniques can be used to compute the energy for parallel plates with mixed (Robin) boundary conditions [18]. For brevity we only quote the results [38]. The energy is

$$\begin{aligned}
\mathcal{E}_{\parallel}(L) &= \frac{\hbar c}{L^3}\Phi(\lambda_1/L, \lambda_2/L),\\
\Phi(\lambda_1/L, \lambda_2/L) &= \frac{1}{4\pi^2}\int_0^{\infty} du u^2\\
&\quad \times \ln\left[1 - \frac{(1-u\lambda_1/L)(1-u\lambda_2/L)}{(1+u\lambda_1/L)(1+u\lambda_2/L)}e^{-2u}\right],
\end{aligned} \tag{4.23}$$

and the force per area is

$$\mathcal{F}_{\parallel}(L) = \frac{\hbar c}{L^4}\Phi'(\lambda_1/L, \lambda_2/L),$$

$$\Phi'(\lambda_1/L, \lambda_2/L) = \frac{1}{2\pi^2}\int_0^\infty du u^3 \times\left[1 - \frac{(1+u\lambda_1/L)(1+u\lambda_2/L)}{(1-u\lambda_1/L)(1-u\lambda_2/L)}e^{2u}\right]^{-1}. \tag{4.24}$$

The amplitudes $\Phi(\lambda_1/L, \lambda_2/L)$, $\Phi'(\lambda_1/L, \lambda_2/L)$ are finite for all $\lambda_\alpha/L \geq 0$. In general, the integrals in Eqs. (4.23) and (4.24) have to be computed numerically. The PFA predictions as functions of $\lambda_{1,2}$ have considerable structure, which we illustrate in Fig. 3.

The behavior of the PFA at asymptotically small or large λ_α/L determines the Casimir interaction as $L \to 0$. For all nonzero values of $\lambda_{1,2}$, we take $\lambda_\alpha/L \to \infty$, but for the Dirichlet case, $\lambda = 0$, the limit $\lambda_\alpha/L \to 0$ applies. For parallel plates with Robin boundary conditions, in the limit $\lambda_{1,2}/L \gg 1$ we obtain the result for Neumann boundary conditions on both plates,

$$\Phi(\lambda_1/L, \lambda_2/L) \to \Phi_0^- = -\frac{\pi^2}{1440}, \tag{4.25}$$

and for $\lambda_{1,2}/L \ll 1$ we obtain the identical result for plates with Dirichlet conditions. Finally for $\lambda_{1,2}/L \ll 1 \ll \lambda_{2,1}/L$, we obtain the parallel plate result for unlike (Dirichlet/Neumann) boundary conditions,

$$\Phi(\lambda_1/L, \lambda_2/L) \to \Phi_0^+ = -\frac{7}{8}\Phi_0^- = \frac{7\pi^2}{11\,520}. \tag{4.26}$$

The last case is relevant at short distances if one of the $\lambda_\alpha = 0$. For two spheres of radius R and center-to-center separation d with Robin boundary conditions, the PFA results can now be obtained easily from Eq. (4.22). In terms of the surface-to-surface distance $L = d - 2R$, we get

$$\mathcal{E}_{\mathrm{PFA}} = \Phi_0^{\pm}\frac{\pi}{2}\frac{R\hbar c}{(d-2R)^2}, \tag{4.27}$$

where the $+$ applies if one and only one $\lambda_\alpha = 0$, and the $-$ in all other cases. Hence, at small separation the interaction becomes independent of λ_α, in the sense that it only depends on whether one λ_α is zero. In fact, the form of the $\mathbb{T}$-matrix of Eq. (4.4) shows that the energy becomes independent of λ_α for $d \ll \min(\lambda_1, \lambda_2)$. Indeed, if we write the frequency as $\kappa = u/d$, the translation matrix depends only on u, and the $\mathbb{T}$-matrix can be written as

$$\mathcal{T}^{\alpha}_{lmlm} = (-1)^l\frac{\pi}{2}\frac{(d/\lambda_\alpha + d/2R_\alpha)I_{l+1/2}(uR_\alpha/d) - uI'_{l+1/2}(uR_\alpha/d)}{(d/\lambda_\alpha + d/2R_\alpha)K_{l+1/2}(uR_\alpha/d) - uK'_{l+1/2}(uR_\alpha/d)}, \tag{4.28}$$

so that the energy depends only on d/R_α for $d \ll \lambda_\alpha$. This universal behavior is confirmed by a numerical evaluation of the energy that is described below.

With the results obtained above, we can analyze the sign of the interaction between plates and spheres at both asymptotically large and small distances. Since the PFA result is expected to hold in the limit where the distance tends to zero, Eq. (4.27) predicts the sign of the interaction between spheres in the limit of vanishing distance. In the limit of large distances, we can compare the results for parallel planes from Eqs. (4.25) and (4.26) to our calculations for two spheres. We find that the *sign* of the

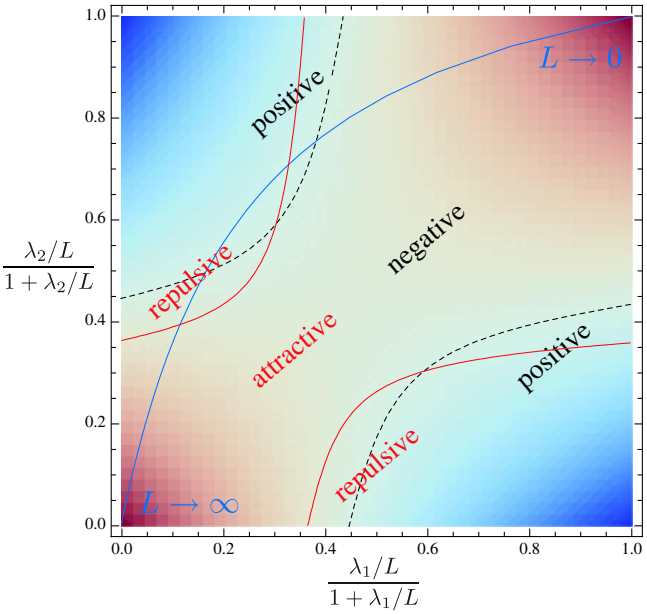

FIG. 3 (color online). Amplitudes $\Phi(\lambda_1/L, \lambda_2/L)$ of the Casimir energy [from Eq. (4.23)] and $\Phi'(\lambda_1/L, \lambda_2/L)$ of the Casimir force [from Eq. (4.24)] for two parallel plates of distance L with Robin boundary conditions. $L = 0$ corresponds to the point (1, 1) unless one or both plates have Dirichlet ($\lambda_\alpha = 0$) boundary conditions. The color coding corresponds to the magnitude of the energy amplitude with blue corresponding to positive energy and red to negative. The dashed (black) curves correspond to zero energy while the solid (red) curves represent zero force. The curve running from the origin to (1, 1) shows as an example the interaction energy for $\lambda_2/\lambda_1 = 5$ as function of the distance L. For finite λ_α the interaction is always attractive at asymptotically large and small distances but can be repulsive at intermediate distances if the ratio $\lambda_1/\lambda_2 \gtrsim 2.8$ (or $\lambda_2/\lambda_1 \gtrsim 2.8$). For $\lambda_1 = \lambda_2$ the interaction is always attractive. The amplitudes are independent of L for the special cases where the λ_α are either zero or infinite: The interaction is attractive (negative energy) for $\lambda_1 = \lambda_2 = 0$, $\lambda_1 = \lambda_2 = \infty$ and repulsive (positive energy) for $\lambda_1 = 0$, $\lambda_2 = \infty$ and $\lambda_1 = \infty$, $\lambda_2 = 0$.

asymptotic interaction depends on the choice for λ_α and is *identical* for plates and spheres. Hence, we obtain a complete characterization of the sign of the interaction at asymptotically large and small distances for the plate and sphere geometry, which is summarized in Table I. However, as we have seen above, the power law decay at large distance is quite different for plates and spheres.

2. Casimir forces for all separations

To go beyond the analytic large distance expansion, we compute numerically the interaction between two spheres of the same radius R with Robin boundary conditions. Guided by the classification of the Casimir force according to its sign at small, intermediate and large separations, we discuss the six different cases listed in Table I. Our numerical approach starts from Eq. (4.1). Using the matrix elements of Eq. (4.4) and (4.5), we compute the determinant and the integral over imaginary frequency numerically. We truncate the matrices at a finite multipole order l so that they have dimension $(1 + l)^2 \times (1 + l)^2$, yielding a series of estimates $\mathcal{E}^{(l)}$ for the Casimir energy.

$\mathcal{E}^{(1)}$ gives the exact result for asymptotically large separations, while for decreasing separations an increasing number of multipoles has to be included. The exact Casimir energy at all separations is obtained by extrapolating the series $\{\mathcal{E}^{(l)}\}$ to $l \to \infty$. We observe an exponentially fast convergence as $|\mathcal{E}^{(l)} - \mathcal{E}| \sim e^{-\delta(d/R-2)l}$, where δ is a constant of order unity. Hence, as the surfaces approach each other for $d \to 2R$, the rate of convergence tends to zero. However, we find that the first $l = 20$ elements of the series are sufficient to obtain accurate results for the energy at a separation with $R/d = 0.48$, corresponding to a surface-to-surface distance of the spheres of $L = 0.083R$, i.e., approximately 4% of the sphere diameter. In principle our approach can be extended to even smaller separations by including higher order multipoles. However, at such small separations semiclassical approximations like the PFA start to become accurate and can be also used.

The results for Dirichlet and Neumann boundary conditions are shown in Fig. 4. All energies are divided by $\mathcal{E}_{\mathrm{PFA}}$, given in Eq. (4.27), with the corresponding amplitude Φ_0^+ (repulsive at small separations) or Φ_0^- (attractive at small separations). For like boundary conditions, either Dirichlet or Neumann, the interaction is attractive at all separations, but for unlike boundary conditions it is repulsive. At large separations the numerical results show excellent agreement with the asymptotic expansion derived above. Note that the reduction of the energy compared to the PFA estimate at large distances depends strongly on the boundary conditions, showing the different power laws at asymptotically large separations. In the limit of a vanishing surface-to-surface distance ($R/d \to 1/2$), the energy approaches the PFA estimate in all cases. Generically, the PFA overestimates the energy: $\mathcal{E}_{\mathrm{PFA}}$ is approached from below for $R/d \to 1/2$, except in the case of Dirichlet boundary conditions on both spheres, where the PFA underestimates the actual energy in a range of $0.3 \lesssim R/d < 1/2$. The deviations from the PFA are most pronounced for Neumann boundary conditions. At a surface-to-surface distance of $L = 3R$ ($R/d = 0.2$), the PFA overestimates the energy by a factor of 100.

Casimir interactions for Robin boundary conditions with finite λ_α are shown in Fig. 5. If $\lambda_1 = \lambda_2$ the interaction is always attractive. If the λ_α are not equal and their ratio is sufficiently large, the Casimir force changes sign either once or twice. This behavior resembles the interaction of two plates with Robin boundary conditions. However, the criterion for the existence of sign changes in the force now depends not only on λ_1/λ_2, but on both quantities λ_1/R and λ_2/R separately. Even with λ_1/λ_2 fixed, for smaller λ_α/R there can be sign changes in the force, while for larger λ_α/R the force is attractive at all distances. When the ratio λ_1/λ_2 is sufficiently large (or formally infinite for Dirichlet or Neumann boundary conditions), we can identify three different generic cases where sign changes in the force occur:

(i) First, we consider Dirichlet boundary conditions ($\lambda_1 = 0$) on one sphere and a finite nonvanishing λ_2/R at the other sphere. Figure 5(a) displays the energy for $\lambda_2/R = 10$ as a typical example. At large distances the energy is negative, while it is positive at short separations with one sign change in between. The asymptotic expansion of Eq. (4.9) with the coefficients of Eq. (4.17) yields the exact energy at separations well below the sign change. While the

TABLE I. The sign of the Casimir force between two plates and two spheres with Robin boundary conditions at asymptotically small and large surface-to-surface distance L. The sign in these two limits is identical for plates and spheres. Here "$-$" and "$+$" indicate attractive and repulsive forces, respectively.

λ_1	λ_2	$L \to 0$	$L \to \infty$	remark
0	0	$-$	$-$	$-$ for all L
∞	0	$+$	$+$	$+$ for all L
∞	∞	$-$	$-$	$-$ for all L
$]0, \infty[$	$]0, \infty[$	$-$	$-$	$+$ at intermediate L for large enough ratio of λ_1, λ_2. (for plates: λ_1/λ_2 or $\lambda_2/\lambda_1 \gtrsim 2.8$)
$]0, \infty[$	0	$+$	$-$	
$]0, \infty[$	∞	$-$	$+$	

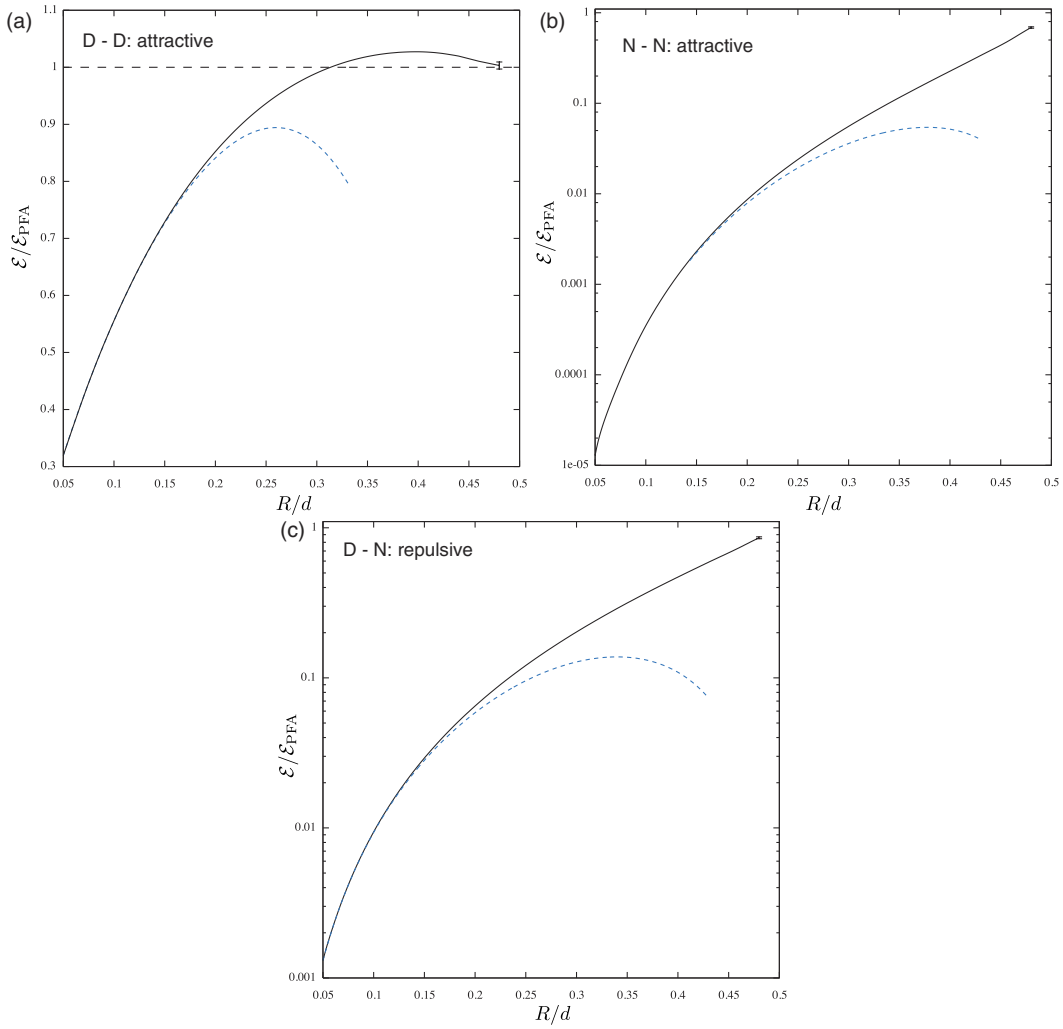

FIG. 4 (color online). Casimir energy for two spheres of radius R and center-to-center distance d: (a) Dirichlet boundary conditions for both spheres, (b) Neumann boundary conditions for both spheres, (c) Spheres with different boundary conditions (one Dirichlet, one Neumann). The energy is scaled by the PFA estimate of Eq. (4.27). The solid curves are obtained by extrapolation to $l \to \infty$. For the smallest separation, the extrapolation uncertainty is maximal and indicated by an error bar. The dashed curves represent the asymptotic large distance expansion given in Eq. (4.9) with the coefficients of Eqs. (4.13), (4.14), and (4.16), respectively.

expansion predicts qualitatively the correct overall behavior of the energy, it does not yield the actual position of the sign change correctly. Of course, for the Casimir interaction between compact objects, the sign of the force $\mathcal{F} = -\partial\mathcal{E}/\partial d$ is the physically important quantity, not the energy. The distance at which the force vanishes cannot be deduced directly from the slope of the curve for $\hat{\mathcal{E}} \equiv \mathcal{E}/\mathcal{E}_{\rm PFA}$, since one has

$$\hat{\mathcal{E}}'(d) = \frac{1}{\mathcal{E}_{\rm PFA}(d)}\left[\mathcal{E}'(d) + \frac{2}{d-2R}\mathcal{E}(d)\right]. \quad (4.29)$$

The force vanishes at the distance d_0 if $\mathcal{E}'(d_0) = 0$, so that

$$\hat{\mathcal{E}}'(d_0) = \frac{2}{d_0 - 2R}\hat{\mathcal{E}}(d_0). \quad (4.30)$$

Hence the distance at which the force vanishes is determined by the position d_0 where the curve of the auxiliary function $t(d) = \tau(d/R - 2)^2$ is tangent to the curve of $\hat{\mathcal{E}}$. The two unknown quantities d_0 and τ are then determined by the conditions $\hat{\mathcal{E}}(d_0) = t(d_0)$ and $\hat{\mathcal{E}}'(d_0) = t'(d_0)$. This procedure allows us to obtain the distance at which the force vanishes easily, without computing derivatives numerically. The tangent segment of the curve for $t(d)$ is shown in Fig. 5(a) as a dotted line. From this construction we find that at a distance $d_{-\Rightarrow+}$ the force changes from attractive to repulsive for decreasing separations. The position $d_{-\Rightarrow+}$ corresponds to a minimum of the energy and decreases with decreasing λ_2/R, so that in the limit $\lambda_2/R \to 0$ it approaches the case of two spheres with Dirichlet boundary conditions,

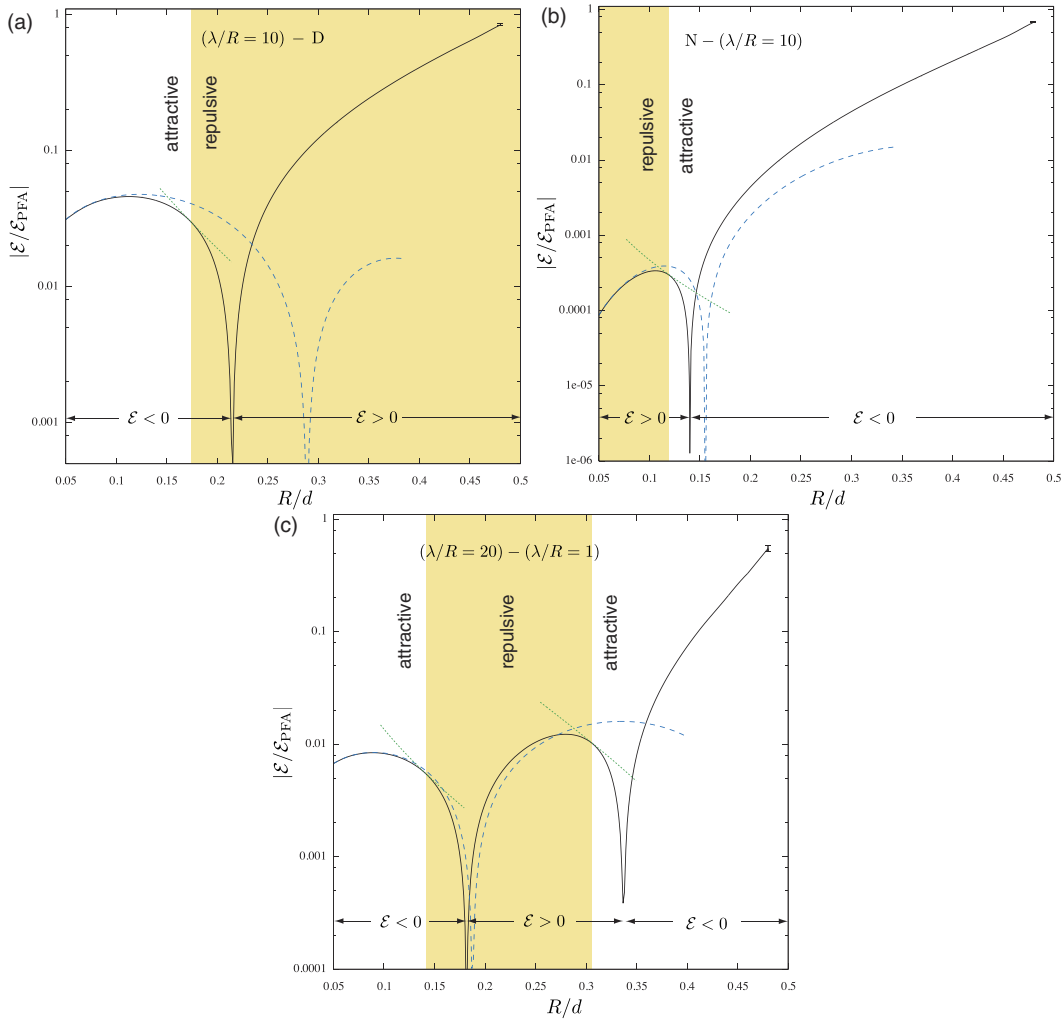

FIG. 5 (color online). The Casimir energy for two spheres with different Robin boundary conditions for finite λ_α: (a) Dirichlet boundary conditions and $\lambda/R = 10$, (b) Neumann boundary conditions and $\lambda/R = 10$, (c) $\lambda_1/R = 10$ and $\lambda_2/R = 1$. The solid curves correspond to extrapolated results for $l \to \infty$, and the dashed curves represent the asymptotic large distance expansion given in Eq. (4.9) with the coefficients of Eqs. (4.17), (4.15), and (4.10), respectively. For logarithmic plotting, the modulus of the energy is shown, and the sign of the energy is indicated at the bottom. The range of separations with a repulsive force is shaded. The points of vanishing force occur where an auxiliary function (dotted curves) is tangent to the solid curve, see text for details.

where the force is always attractive.

(ii) Second, we study Neumann boundary conditions on one sphere and a finite nonvanishing λ_2/R at the other sphere. As an example we choose again $\lambda_2/R = 10$, as shown in Fig. 5(b). The energy is positive at large distances and becomes negative at small distances. The asymptotic expansion with the coefficients of Eq. (4.15) is found to be valid well below the separation where the sign of the energy changes. Hence, the expansion describes the behavior of the energy qualitatively, but does not predict the precise position of the sign change. The sign change of the force can be obtained by the method described above. At a position $d_{+\Rightarrow-}$, the force changes from repulsive to attractive with decreasing separation and the energy is maximal. A decreasing (increasing) λ_2/R shifts $d_{+\Rightarrow-}$ to smaller (larger) separations. This result is consistent with an entirely repulsive (attractive) force for Neumann-Dirichlet (Neumann-Neumann) boundary conditions.

(iii) The third case is obtained if both λ_α are finite and nonzero. A typical example with $\lambda_1/R = 20$ and $\lambda_2/R = 1$ is shown in Fig. 5(c). The energy is negative both at large and small separations but turns positive at intermediate distances. The asymptotic expansion applies again at sufficiently large separations beyond the position where the energy becomes positive. For values of the ratio λ_1/λ_2 that are larger than an R-dependent threshold, the force changes sign twice, so that it is repulsive between the separations $d_{-\Rightarrow+}$ and $d_{+\Rightarrow-}$. The energy has a minimum (maximum) at $d_{-\Rightarrow+}$ ($d_{+\Rightarrow-}$). If λ_1/R increases and

λ_2/R decreases, the repulsive region grows until eventually the force becomes repulsive at all separations, corresponding to the limit of Dirichlet/Neumann boundary conditions. Decreasing λ_1/R and increasing λ_2/R reduces the interval with repulsion. In this case, first the zeros of the energy disappear, leaving negative energy at all distances but still a repulsive region, and then the two positions where the force vanishes merge, leaving an entirely attractive force.

D. Interaction in terms of low frequency scattering data

We noted in Sec. II C that in the limit of vanishing frequency, the $\mathbb{S}$-matrix is related to tensor generalizations of the capacitance. At higher frequencies, this tensor receives corrections that can be expanded in frequency. The object's shape is thus encoded in the tensor expansion coefficients of the $\mathbb{S}$-matrix. We can use these results to obtain the Casimir interaction between nonspherical objects in a large distance expansion. From such an analysis one can obtain information about which pieces of the $\mathbb{S}$-matrix contribute to the Casimir interaction at a given order in inverse separation.

In general, according to Eq. (2.29), the $\mathbb{T}$-matrix of object α can be written in a small κ-expansion of the form

$$\mathcal{T}^{\alpha}_{l'm'lm} = \frac{i^{l+l'}}{(2l+1)!!(2l'-1)!!}\sum_{q=0}^{\infty} C^{\alpha}_{q;l'm'lm}\kappa^{l+l'+1+q}. \tag{4.31}$$

Because of the symmetry of the $\mathbb{T}$-matrix, the coefficients obey the relation

$$C^{\alpha}_{q;l'm'lm} = \frac{2l+1}{2l'+1}C^{\alpha}_{q;lml'm'}. \tag{4.32}$$

We assume again that the origins of the two objects are located on the z-axis at a separation d. Then we can use the translation matrix elements of Eq. (4.5). The Casimir energy can be obtained from the low-κ expression for the $\mathbb{T}$-matrix of Eq. (4.31) by a simultaneous expansion in the number of partial waves, the number of scatterings (powers of $\mathbb{N}$), and the imaginary frequency κ. The analysis based on the general low-frequency structure of the $\mathbb{T}$-matrix for objects of arbitrary shape and boundary condition becomes increasingly complicated with decreasing separation between the objects. Since the $\mathbb{T}$-matrix cannot be assumed to be diagonal in l, partial waves of order l can contribute to the energy at order $d^{-(3+l)}$ (for $\mathbb{T}$-matrices that are diagonal in l, they can only contribute at order $d^{-(3+2l)}$). We consider here only partial waves up to order $l = 3$ and four scatterings, which allows us to obtain the energy to order d^{-6}. The energy can again be written in the form

$$\mathcal{E} = \frac{\hbar c}{\pi}\sum_{j=3}^{\infty}\frac{B_j}{d^j}. \tag{4.33}$$

The coefficients B_j are completely specified by the low-frequency behavior of the $\mathbb{T}$-matrix, i.e., they can be obtained from the coefficients $C^{\alpha}_{q;l'm'lm}$ in Eq. (4.31). In the following, we assume that the origin of the object's coordinate frame has been chosen such that the dipole response to an applied constant potential vanishes, i.e., $C^{\alpha}_{0;1m00} = C^{\alpha}_{0;001m} = 0$ for $m = -1, 0, 1$. Using the symmetry relation of Eq. (4.32), the result for the coefficients can be written as

$$B_3 = -\tfrac{1}{4}C^1_{0;0000}C^2_{0;0000}, \tag{4.34}$$

$$B_4 = -\tfrac{1}{8}(C^1_{0;0000}C^2_{1;0000} + C^2_{0;0000}C^1_{1;0000}), \tag{4.35}$$

$$\begin{aligned} B_5 = &-\frac{1}{16}[C^1_{0;0000}C^2_{0;0000}]^2 - \frac{5}{8}(C^1_{0;0000}C^2_{0;1010} + C^2_{0;0000}C^1_{0;1010}) - \frac{\sqrt{5}}{6}(C^1_{0;0020}C^2_{0;0000} + C^2_{0;0020}C^1_{0;0000}) \\ &- \frac{1}{2\sqrt{3}}(C^1_{0;0000}C^2_{1;0010} - C^2_{0;0000}C^1_{1;0010}) - \frac{1}{8}(C^1_{1;0000}C^2_{1;0000} + C^1_{0;0000}C^2_{2;0000} + C^2_{0;0000}C^1_{2;0000}), \end{aligned} \tag{4.36}$$

$$\begin{aligned} B_6 = &-\frac{1}{32}(C^1_{0;0000}C^1_{1;0000}[C^2_{0;0000}]^2 + C^2_{0;0000}C^2_{1;0000}[C^1_{0;0000}]^2) - \frac{7}{8}\sqrt{\frac{5}{3}}(C^1_{0;0000}C^2_{0;1020} - C^2_{0;0000}C^1_{0;1020}) \\ &- \frac{\sqrt{7}}{8}(C^1_{0;0000}C^2_{0;0030} - C^2_{0;0000}C^1_{0;0030}) - \frac{9}{16}(C^1_{0;0000}C^2_{1;1010} + C^2_{0;0000}C^1_{1;1010} + C^1_{1;0000}C^2_{0;1010} + C^2_{1;0000}C^1_{0;1010}) \\ &- \frac{\sqrt{5}}{8}(C^1_{1;0020}C^2_{0;0000} + C^2_{1;0020}C^1_{0;0000} + C^1_{1;0000}C^2_{0;0020} + C^2_{1;0000}C^1_{0;0020}) - \frac{5}{8\sqrt{3}}(C^1_{0;0000}C^2_{2;0010} - C^2_{0;0000}C^1_{2;0010} \\ &+ C^1_{1;0000}C^2_{1;0010} - C^2_{1;0000}C^1_{1;0010}) - \frac{3}{16}(C^1_{1;0000}C^2_{2;0000} + C^2_{1;0000}C^1_{2;0000} + C^1_{0;0000}C^2_{3;0000} + C^2_{0;0000}C^1_{3;0000}). \end{aligned} \tag{4.37}$$

This result deserves several comments. First, the above expressions for the coefficients have been substantially simplified by the requirement that $C^{\alpha}_{1m00} = C^{\alpha}_{001m} = 0$, which eliminates 2, 5 and 22 terms from B_4, B_5 and B_6, respectively. Most contributions originate from two scatterings, which can be seen from the appearance of a product of two coefficients

$C^{\alpha}_{q;lml'm'}$. Only the leading terms of B_5 and B_6 are composed of a product of four coefficients $C^{\alpha}_{q;lml'm'}$ and hence result from four scatterings. The latter terms are completely determined by the capacitance of the objects and its finite frequency corrections, $C^{\alpha}_{q;0000}$. The result clearly shows the relevant number of partial waves, which increases by one with each additional power of $1/d$. At leading order, $\sim 1/d^3$, the coefficient B_3 is given by the product of the capacitances $C^{\alpha}_{0;0000}$ of the objects. At the next order, contributions from $l = 1$ partial waves are absent due to the choice of origin. At higher orders, the coefficients B_j contain contributions from partial waves up to $l = j - 3$. Note also that not all terms are symmetric under an exchange of the two objects, $C^{1}_{q,lml'm'} \leftrightarrow C^{2}_{q,lml'm'}$. The terms for which $l + l'$ is an odd number change sign under an exchange of the objects. This is related to the fact that the expansion of the $\mathbb{T}$-matrix in Eq. (4.31) assumes that the local coordinate systems of the two objects have the same orientation. Hence, the objects "see" each other along different directions, i.e., along the direction of the positive and negative z-axis, respectively. Up to coefficient B_6, all terms have $m = m' = 0$, which is again due to the choice of origins eliminating all terms with nonzero m up to the order considered here.

The above result can be applied to two objects of arbitrary shape and orientation, since the direction connecting the origins of the objects can be always defined as the z-axis. The orientation of the objects with respect to this axis is then specified by the coefficients $C^{\alpha}_{q,lml'm'}$, which depend on the angle that a reference direction, fixed to the object, forms with the z-axis. Hence, the dependence of the Casimir interaction on the orientation of the objects can be obtained from this general result by computing the low-frequency expansion of the $\mathbb{T}$-matrix elements for objects with an arbitrary orientation with respect to the z-axis. Since the capacitance coefficients $C^{\alpha}_{q;0000}$ are independent of orientation, a dependence on orientation can occur only at order d^{-5}. A more detailed study of the orientation dependence and the reduction of the number of independent expansion coefficients due to symmetries of the objects is left to a future publication.

ACKNOWLEDGMENTS

This work was supported by the National Science Foundation (NSF) through grants DMR-04-26677 (M. K.) and PHY-0555338 (N. G.), by Research Corporation (N. G.), by the U. S. Department of Energy (DOE) under cooperative research agreement #DF-FC02-94ER40818 (R. L. J.), and the German Research Foundation (T. E.).

APPENDIX A: NEUMANN BOUNDARY CONDITIONS

Throughout the paper we considered Dirichlet boundary conditions, $\phi = 0$. In fact, our final result, Eq. (3.25), which expresses the interaction Casimir energy of many compact objects in terms of the transition and translation matrices, is independent of the choice of boundary conditions, provided the $\mathbb{T}$-matrix is the one appropriate to the boundary conditions of interest. Here we show this result for the Neumann case. The general Robin case is left to the reader.

Neumann boundary conditions are implemented by replacing $\phi(\mathbf{x})$ by $\partial_n \phi(\mathbf{x})$ in Eq. (2.12), leading to an expression for the partition function analogous to Eq. (2.13) with $\phi(\mathbf{x}) \to \partial_n \phi(\mathbf{x})$. Like the Dirichlet case, this case also has an analogy to electrostatics, namely, a complex field coupled to a set of *surface dipole densities* $\varrho_\alpha(\mathbf{x})$. By analogy, in this case $\partial_n \phi$ will be continuous throughout space, but ϕ itself will jump by $\varrho_\alpha(\mathbf{x})$ across the surface Σ_α. Therefore the classical equations of motion analogous to Eq. (3.1) are

$$\begin{aligned} -(\nabla^2 + k^2)\phi_{\mathrm{cl}}(\mathbf{x}) &= 0, \quad \text{for } \mathbf{x} \notin \Sigma_\alpha, \\ \Delta\phi_{\mathrm{cl}}(\mathbf{x}) &= -\varrho_\alpha(\mathbf{x}), \quad \text{for } \mathbf{x} \in \Sigma_\alpha, \\ \Delta\partial_n\phi_{\mathrm{cl}}|_{\mathbf{x}} &= 0, \quad \text{for } \mathbf{x} \in \Sigma_\alpha, \end{aligned} \tag{A1}$$

and the normal derivative of the free Green's function generates the field associated with these dipole sources,

$$\phi_{\mathrm{cl}}(\mathbf{x}) = \sum_\beta \int_{\Sigma_\beta} d\mathbf{x}' \partial_{n'} \mathcal{G}_0(\mathbf{x}, \mathbf{x}', k) \varrho_\beta(\mathbf{x}'), \tag{A2}$$

where $\partial_{n'}$ denotes the normal derivative at the point $\mathbf{x}'$ and acts only on $\mathcal{G}_0$.

The evaluation of the classical action proceeds in analogy to the Dirichlet case,

$$\tilde{S}_{\mathrm{cl}}[\varrho] = \frac{1}{2}\sum_{\alpha,\beta}\left(\int_{\Sigma_\alpha} d\mathbf{x} \varrho^*_\alpha(\mathbf{x}) \partial_n \phi_\beta(\mathbf{x}) + \text{c.c.}\right). \tag{A3}$$

First we evaluate the terms with $\alpha \neq \beta$,

$$\tilde{S}_{\beta\alpha} = \frac{1}{2}\int_{\Sigma_\alpha} d\mathbf{x} (\varrho^*_\alpha(\mathbf{x}) \partial_n \phi_\beta(\mathbf{x}) + \text{c.c.}). \tag{A4}$$

In analogy to Eq. (3.9),

$$\begin{aligned} \phi_\beta(\mathbf{x}) = ik \sum_{lm} h^{(1)}_l(kr_\beta) Y_{lm}(\hat{\mathbf{x}}_\beta) \\ \times \int_{\Sigma_\beta} d\mathbf{x}'_\beta \partial_{n'} [j_l(kr'_\beta) Y^*_{lm}(\hat{\mathbf{x}}'_\beta)] \varrho_\beta(\mathbf{x}'_\beta), \end{aligned} \tag{A5}$$

which serves to define multipole moments of the dipole layer density,

$$P_{\beta,lm} \equiv \int_{\Sigma_\beta} d\mathbf{x}_\beta \partial_n [j_l(kr_\beta) Y^*_{lm}(\hat{\mathbf{x}}_\beta)] \varrho_\beta(\mathbf{x}_\beta). \tag{A6}$$

As in the Dirichlet case, the Hankel functions defined with respect to $\mathcal{O}_\beta$ can be expanded in terms of Bessel functions about $\mathcal{O}_\alpha$ with the help of translation formulas. Substituting into Eq. (A4) leads to a result analogous to

Eq. (3.13),

$$\tilde{S}_{\beta\alpha}[P_\alpha, P_\beta] = \frac{ik}{2} \sum_{lml'm'} P^*_{\alpha,l'm'} \mathcal{U}^{\alpha\beta}_{l'm'lm} P_{\beta,lm} + \text{c.c.}. \quad \text{(A7)}$$

When $\alpha = \beta$, we also proceed in analogy to the Dirichlet case. The interior field is defined as in Eq. (3.15) and substitution into Eq. (A3) leads to

$$\tilde{S}_\alpha[\varrho_\alpha] = \frac{1}{2} \sum_{lm} (\phi_{\alpha,lm} P^*_{\alpha,lm} + \text{c.c.}), \quad \text{(A8)}$$

in analogy to Eq. (3.16). As in the Dirichlet case, we determine the field expansion coefficients, $\phi_{\alpha,lm}$, by constructing the exterior field $\phi_{\text{out},\alpha}$ in two different ways. First we construct it following the logic of Eqs. (3.17), (3.18), (3.19), and (3.20), but now with the aid of the *Neumann* $\mathbb{T}$-matrix, since the normal derivative of ϕ_α must be continuous across Σ_α. Then we construct $\phi_{\text{out},\alpha}$ directly from the Neumann multipole moments using Eq. (A2). Equating the two we obtain

$$\phi_{\alpha,lm} = -ik \sum_{l'm'} [\mathcal{T}^\alpha]^{-1}_{lml'm'} P_{\alpha,l'm'}, \quad \text{(A9)}$$

where $\mathcal{T}^\alpha$ is the Neumann $\mathbb{T}$-matrix. Substituting into Eq. (A8) we obtain the final result,

$$\tilde{S}_\alpha[P_\alpha] = -\frac{ik}{2} \sum_{lm} P^*_{\alpha,lm} [\mathcal{T}^\alpha]^{-1}_{lml'm'} P_{\alpha,l'm'} + \text{c.c.}, \quad \text{(A10)}$$

analogous to Eq. (3.22). The rest of the derivation follows the Dirichlet case closely.

APPENDIX B: CASIMIR ENERGY AND FUNCTIONAL INTEGRALS

Here we show the equivalence between our functional integral formalism and the standard representation of the Casimir energy in terms of zero-point energies. We consider a real scalar field, $\varphi(\mathbf{x}, t)$, that obeys the wave equation in a domain $\mathcal{D}$, and obeys a Dirichlet boundary condition on Σ, the boundary of $\mathcal{D}$, which need not be connected. Let $\phi_\alpha(\mathbf{x})$ and $-\varepsilon_\alpha^2/\hbar^2c^2$ be the eigenfunctions and eigenvalues of the Laplacian in $\mathcal{D}$,

$$\begin{aligned} -\nabla^2 \phi_\alpha(\mathbf{x}) &= \frac{\varepsilon_\alpha^2}{\hbar^2 c^2} \phi_\alpha(\mathbf{x}) \quad \text{in } \mathcal{D}, \\ \phi_\alpha(\mathbf{x}) &= 0 \quad \text{on } \Sigma. \end{aligned} \quad \text{(B1)}$$

Let $-\varepsilon_{\infty,\alpha}^2/\hbar^2c^2$ be the corresponding eigenvalues when the objects are moved to arbitrarily large separation from one another. For simplicity we assume that the spectrum is discrete in both cases.

Consider the Minkowski space functional integral over the field $\varphi(\mathbf{x}, t)$, as introduced in Eq. (2.1) but now for a real field,

$$Z[\mathcal{C}] = \int [\mathcal{D}\varphi]_{\mathcal{C}} \exp\left\{\frac{i}{\hbar} \int_0^T dt \int_{\mathcal{D}} d\mathbf{x} \left(\frac{1}{c^2} (\partial_t \varphi)^2 - (\nabla\varphi)^2\right)\right\}. \quad \text{(B2)}$$

By definition, only periodic paths, $\varphi(\mathbf{x}, 0) = \varphi(\mathbf{x}, T)$, that obey the Dirichlet boundary conditions are included. Since $\varphi(\mathbf{x}, t)$ is periodic in T, it can be expanded in a Fourier series,

$$\varphi(\mathbf{x}, t) = \sum_{n=-\infty}^{\infty} \varphi_n(\mathbf{x}) e^{-2\pi nit/T},$$

with $\varphi_{-n}(\mathbf{x}) = \varphi_n^*(\mathbf{x})$. Because the boundary conditions are time independent, the functional integral over each frequency mode of φ can be done independently. Therefore $Z[\mathcal{C}]$ can be written as an infinite product,

$$Z[\mathcal{C}] = \prod_{n=-\infty}^{\infty} \int [\mathcal{D}\varphi_n]_{\mathcal{C}} \exp\left\{\frac{iT}{\hbar} \int_{\mathcal{D}} d\mathbf{x} \left(\left(\frac{2\pi n}{cT}\right)^2 |\varphi_n|^2 - |\nabla\varphi_n|^2\right)\right\}. \quad \text{(B3)}$$

At the end of this calculation we will divide by Z_∞, the functional integral defined when all the objects are removed to arbitrarily large separation. Therefore we ignore all multiplicative factors in $Z[\mathcal{C}]$ that are independent of the location of the constraining surfaces, beginning with the Jacobian generated by the change of variables from $\varphi(\mathbf{x}, t)$ to $\varphi_n(\mathbf{x})$.

The real eigenfunctions, $\{\phi_\alpha(\mathbf{x})\}$, defined in Eq. (B1) form a complete orthonormal set of functions on $\mathcal{D}$, so the field $\varphi_n(\mathbf{x})$ can be expanded as

$$\varphi_n(\mathbf{x}) = \sum_\alpha c_{n\alpha} \phi_\alpha(\mathbf{x}),$$

where $\{c_{n\alpha}\}$ are complex numbers with $c_{-n\alpha} = c_{n\alpha}^*$. When this expansion is substituted into $Z[\mathcal{C}]$, the functional integral reduces to an infinite product of ordinary integrals over the coefficients $\{c_{n\alpha}\}$,

$$Z[\mathcal{C}] = \prod_{n=-\infty}^{\infty} \prod_\alpha \int dc_{n\alpha} \exp\left\{-\frac{iT}{\hbar} \sum_\alpha \left(\frac{\varepsilon_\alpha^2}{\hbar^2 c^2} - \left(\frac{2\pi n}{cT}\right)^2\right) |c_{n\alpha}|^2\right\}, \quad \text{(B4)}$$

where we have dropped factors common to $Z[\mathcal{C}]$ and Z_∞. The integrals over the $\{c_{n\alpha}\}$ can be performed (taking T complex with a negative imaginary part, and analytically continuing back to T real at the end), leading to

$$Z[\mathcal{C}] = \prod_{n=-\infty}^{\infty} \prod_\alpha \left(\frac{\varepsilon_\alpha^2}{\hbar^2 c^2} - \left(\frac{2\pi n}{cT}\right)^2\right)^{-1/2}. \quad \text{(B5)}$$

Then, interchanging the products over n and α, $Z[\mathcal{C}]$ can be written,

$$Z[\mathcal{C}] = \prod_\alpha \frac{\hbar c}{\varepsilon_\alpha} \prod_{n=1}^{\infty} \left[\frac{\varepsilon_\alpha^2}{\hbar^2 c^2} - \left(\frac{2\pi n}{cT}\right)^2 \right]^{-1}, \tag{B6}$$

where we have separated out the $n = 0$ term and combined each positive and negative n into a single term. Factoring out the configuration independent factor $\prod_{n=1}^{\infty}(\frac{2\pi n}{cT})^2$ and using the infinite product representation of the sine function,

$$\frac{\sin x}{x} = \prod_{n=1}^{\infty}\left(1 - \frac{x^2}{\pi^2 n^2}\right),$$

we obtain

$$Z[\mathcal{C}] = \prod_\alpha \frac{1}{\sin\frac{\varepsilon_\alpha T}{2\hbar}} = \prod_\alpha \frac{e^{-i(\varepsilon_\alpha T/2\hbar)}}{1 - e^{-i(\varepsilon_\alpha T/\hbar)}}. \tag{B7}$$

Finally we define $T = -i\Lambda/c$, send $\Lambda \to \infty$, divide by Z_∞, and take the logarithm, obtaining

$$\lim_{\Lambda\to\infty} \ln(Z[\mathcal{C}]/Z_\infty) = -\frac{\Lambda}{2\hbar c}\sum_\alpha (\epsilon_\alpha - \epsilon_{\alpha,\infty}), \tag{B8}$$

which, using Eq. (2.4), gives the standard expression for the Casimir energy of a real scalar field,

$$\mathcal{E}[\mathcal{C}] = \frac{1}{2}\sum_\alpha (\varepsilon_\alpha - \varepsilon_{\infty,\alpha}). \tag{B9}$$

Note that if we had set $T = -i\beta\hbar$ and not taken the $T \to \infty$ limit, we would have obtained the partition function for a Bose "gas" of scalar particles occupying the eigenstates with energy ε_α, the starting point for a quantum statistical mechanical treatment of the Casimir effect at temperature $1/\beta$.

APPENDIX C: TRANSLATION FORMULAS

For completeness, we sketch the derivations of the translation formulas quoted in Eqs. (2.30) and (2.31) with $\beta = 1$ and $\alpha = 2$. See Fig. 1 for the configuration of the two objects.

1. $\mathcal{V}^{12}_{l'm'lm}(\mathbf{X}_{12})$

First consider the equation relating the regular partial wave solution about $\mathbf{x}_2$ to those expanded about $\mathcal{O}_1$. Since $\mathbf{x}_2 = \mathbf{X}_{21} + \mathbf{x}_1$ we can write

$$e^{i\mathbf{k}\mathbf{x}_2} = e^{i\mathbf{k}\mathbf{X}_{21}} e^{i\mathbf{k}\mathbf{x}_1}, \tag{C1}$$

for an arbitrary vector $\mathbf{k}$. If we use the familiar partial wave expansion,

$$e^{i\mathbf{k}\mathbf{x}} = 4\pi \sum_{lm} i^l j_l(kr) Y^*_{lm}(\hat{\mathbf{k}}) Y_{lm}(\hat{\mathbf{x}}), \tag{C2}$$

in all three terms, multiply by the factor $Y_{lm}(\mathbf{k})$ and integrate over $\hat{\mathbf{k}}$, we obtain

$$\begin{aligned} j_l(kr_2)Y_{lm}(\hat{\mathbf{x}}_2) = 4\pi \sum_{l'm'l''m''} i^{l'+l''-l} \Big(\int d\hat{\mathbf{k}}\, Y_{lm}(\hat{\mathbf{k}}) Y^*_{l'm'}(\hat{\mathbf{k}}) \\ \times Y^*_{l''m''}(\hat{\mathbf{k}}) \Big) j_{l''}(kd_{12}) j_{l'}(kr_1) \\ \times Y_{l''m''}(\hat{\mathbf{X}}_{21}) Y_{l'm'}(\hat{\mathbf{x}}_1). \end{aligned} \tag{C3}$$

The integral over three spherical harmonics is [39]

$$\begin{aligned} \int d\hat{\mathbf{k}}\, Y_{lm}(\hat{\mathbf{k}}) Y^*_{l'm'}(\hat{\mathbf{k}}) Y^*_{l''m''}(\hat{\mathbf{k}}) = (-1)^{m'+m''} \\ \times \sqrt{\frac{\lambda\lambda'\lambda''}{4\pi}} \begin{pmatrix} l & l' & l'' \\ 0 & 0 & 0 \end{pmatrix} \\ \times \begin{pmatrix} l & l' & l'' \\ m & -m' & -m'' \end{pmatrix}, \end{aligned} \tag{C4}$$

where $\lambda \equiv 2l + 1$. Substituting into Eq. (C3) and regrouping terms we find,

$$\begin{aligned} j_l(kr_2)Y_{lm}(\hat{\mathbf{x}}_2) = \sum_{l'm'} \Big[\sum_{l''m''} i^{l''} (-1)^{m''} \sqrt{\lambda''} \begin{pmatrix} l & l' & l'' \\ 0 & 0 & 0 \end{pmatrix} \\ \times \begin{pmatrix} l & l' & l'' \\ m & -m' & -m'' \end{pmatrix} j_{l''}(kd_{12}) Y_{l''m''}(\hat{\mathbf{X}}_{21}) \\ \times \sqrt{4\pi\lambda\lambda'}\, i^{l'-l} (-1)^{m'} j_{l'}(kr_1) Y_{l'm'}(\hat{\mathbf{x}}_1) \Big]. \end{aligned} \tag{C5}$$

Comparing this expression with the definition of the translation matrix, $\mathbb{V}$, given in Eq. (2.30), we can read off the matrix elements $\mathcal{V}^{12}_{lml'm'}(\mathbf{X}_{12})$,

$$\begin{aligned} \mathcal{V}^{12}_{l'm'lm}(\mathbf{X}_{12}) = \sqrt{4\pi\lambda\lambda'}\, i^{l'-l} (-1)^{m'} \sum_{l''m''} i^{l''} (-1)^{m''} \\ \times \sqrt{\lambda''} \begin{pmatrix} l & l' & l'' \\ 0 & 0 & 0 \end{pmatrix} \\ \times \begin{pmatrix} l & l' & l'' \\ m & -m' & -m'' \end{pmatrix} j_{l''}(kd_{12}) Y_{l''m''}(\hat{\mathbf{X}}_{21}). \end{aligned} \tag{C6}$$

Finally we use $\hat{\mathbf{X}}_{21} = -\hat{\mathbf{X}}_{12}$ and $Y_{l''m''}(-\hat{\mathbf{X}}) = (-1)^{l''} Y_{l''m''}(\hat{\mathbf{X}})$, together with the fact the the $3j$-symbol restricts $l' + l'' - l$ to be even and $m' + m''$ to equal m, all of which yields

$$\begin{aligned} \mathcal{V}^{12}_{l'm'lm}(\mathbf{X}_{12}) = \sqrt{4\pi\lambda\lambda'}\, i^{l-l'} (-1)^{m} \sum_{l''m''} i^{l''} \sqrt{\lambda''} \begin{pmatrix} l & l' & l'' \\ 0 & 0 & 0 \end{pmatrix} \\ \times \begin{pmatrix} l & l' & l'' \\ m & -m' & -m'' \end{pmatrix} j_{l''}(kd_{12}) Y_{l''m''}(\hat{\mathbf{X}}_{12}), \end{aligned} \tag{C7}$$

the analogue of Eq. (2.31).

2. $\mathcal{U}^{12}_{l'm'lm}(\mathbf{X}_{12})$

We begin by equating the partial wave expansion (with respect to $\mathcal{O}_2$) of the free Green's function to its plane wave representation,

$$\mathcal{G}_0(\mathbf{x}, \mathbf{x}_2, k) = ik\sum_{lm} j_l(kr)h_l^{(1)}(kr_2)Y^*_{lm}(\hat{\mathbf{x}})Y_{lm}(\hat{\mathbf{x}}_2) = \int \frac{d\mathbf{q}}{(2\pi)^3}\frac{e^{i\mathbf{q}(\mathbf{x}_2-\mathbf{x})}}{q^2-k^2}. \tag{C8}$$

Without loss of generality we take $|\mathbf{x}_2| > |\mathbf{x}|$ with respect to $\mathcal{O}_2$. We project out the (lm)th partial wave by multiplying by $Y_{lm}(\hat{\mathbf{x}})$ and integrating over $\hat{\mathbf{x}}$,

$$ikj_l(kr)h_l^{(1)}(kr_2)Y_{lm}(\hat{\mathbf{x}}_2) = \int d\hat{\mathbf{x}}Y_{lm}(\hat{\mathbf{x}})\int\frac{d\mathbf{q}}{(2\pi)^3}\frac{e^{i\mathbf{q}(\mathbf{x}_2-\mathbf{x})}}{q^2-k^2}. \tag{C9}$$

Next we write $e^{i\mathbf{q}(\mathbf{x}_2-\mathbf{x})} = e^{i\mathbf{q}(\mathbf{X}_{21}+\mathbf{x}_1-\mathbf{x})}$ and expand each exponential in partial waves using Eq. (C2). The $\hat{\mathbf{x}}$ integral can be performed using the orthonormality of the Y_{lm}; the $\hat{\mathbf{q}}$ integral is of the form of Eq. (C4). The substitution of $\mathbf{X}_{21} = -\mathbf{X}_{12}$ proceeds as in the previous case and we obtain

$$ikj_l(kr)h_l^{(1)}(kr_2)Y_{lm}(\hat{\mathbf{x}}_2) = \frac{8(-1)^m}{\sqrt{4\pi}}\sum_{l'm'l''m''} i^{l+l''-l'}\sqrt{\lambda\lambda'\lambda''}\begin{pmatrix} l & l' & l'' \\ 0 & 0 & 0\end{pmatrix}\begin{pmatrix} l & l' & l'' \\ m & -m' & -m''\end{pmatrix} \times\left[\int_0^\infty dq\frac{q^2}{q^2-k^2}j_{l''}(qd_{12})j_{l'}(qr_1)j_l(qr)\right]Y_{l''m''}(\hat{\mathbf{X}}_{12})Y_{l'm'}(\hat{\mathbf{x}}_1). \tag{C10}$$

This integral can be found in Ref. [40],

$$\int_0^\infty dq\frac{q^2}{q^2-k^2}j_{l''}(qd_{12})j_{l'}(qr_1)j_l(qr) = \frac{ik\pi}{2}j_l(kr)j_{l'}(kr_1)h^{(1)}_{l''}(kd_{12}). \tag{C11}$$

Substituting this result into Eq. (C10), the form of $\mathcal{U}^{12}_{lml'm'}(\mathbf{X}_{12})$ quoted in Eq. (2.31) follows straightforwardly.

[1] H. B. G. Casimir, Indagationes mathematicae / Koninklijke Nederlandsche Akademie van Wetenschappen **10**, 261 (1948); Kon. Ned. Akad. Wetensch. Proc. **51**, 793 (1948).

[2] N. Graham, R. L. Jaffe, V. Khemani, M. Quandt, O. Schroeder, and H. Weigel, Nucl. Phys. **B677**, 379 (2004); N. Graham, R. L. Jaffe, V. Khemani, M. Quandt, M. Scandurra, and H. Weigel, Nucl. Phys. **B645**, 49 (2002).

[3] See, for example, M. Bordag, U. Mohideen, and V. M. Mostepanenko, Phys. Rep. **353**, 1 (2001).

[4] F. Chen, G. L. Klimchitskaya, V. M. Mostepanenko, and U. Mohideen, Phys. Rev. Lett. **97**, 170402 (2006).

[5] R. S. Decca, D. López, E. Fischbach, G. L. Klimchitskaya, D. E. Krause, and V. M. Mostepanenko, Phys. Rev. D **75**, 077101 (2007).

[6] F. Chen, G. L. Klimchitskaya, V. M. Mostepanenko, and U. Mohideen, Phys. Rev. B **76**, 035338 (2007).

[7] J. N. Munday and F. Capasso, Phys. Rev. A **75**, 060102(R) (2007).

[8] D. E. Krause, R. S. Decca, D. López, and E. Fischbach, Phys. Rev. Lett. **98**, 050403 (2007).

[9] H. B. Chan, V. A. Aksyuk, R. N. Kleiman, D. J. Bishop, and F. Capasso, Phys. Rev. Lett. **87**, 211801 (2001).

[10] F. Capasso, J. N. Munday, D. Iannuzzi, and H. B. Chan, IEEE J. Quantum Electron. **13**, 400 (2007).

[11] T. Emig, N. Graham, R. L. Jaffe, and M. Kardar, Phys. Rev. Lett. **99**, 170403 (2007).

[12] The scattering matrix can be determined either theoretically (numerically or analytically) when there exists an appropriate model for the material, or experimentally by scattering experiments. Developing a suitable theoretical description of a particular material is an important but separate problem. See Refs. [13,14] for a recent discussion.

[13] B. Geyer, G. L. Klimchitskaya, and V. M. Mostepanenko, Phys. Rev. D **72**, 085009 (2005).

[14] V. B. Bezerra, R. S. Decca, E. Fischbach, B. Geyer, G. L. Klimchitskaya, D. E. Krause, D. Lopez, V. M. Mostepanenko, and C. Romero, Phys. Rev. E **73**, 028101 (2006); I. Brevik, J. B. Aarseth, J. S. Hoye, and K. A. Milton, Phys. Rev. E **71**, 056101 (2005).

[15] T. Emig, N. Graham, R. L. Jaffe, and M. Kardar (unpublished).

[16] J. Schwinger, Lett. Math. Phys. **1**, 43 (1975).

[17] M. Bordag, D. Robaschik, and E. Wieczorek, Ann. Phys. (N.Y.) **165**, 192 (1985).

[18] H. Li and M. Kardar, Phys. Rev. Lett. **67**, 3275 (1991); Phys. Rev. A **46**, 6490 (1992).

[19] See, for example, Eqs. (47), (62), (65), (66) in Ref. [20].

[20] R. C. Wittmann, IEEE Trans. Antennas Propag. **36**, 1078 (1988).

[21] See, for example, R. G. Newton, *Scattering Theory of Waves and Particles* (McGraw-Hill, New York, 1966).

[22] H. B. G. Casimir and D. Polder, Phys. Rev. **73**, 360 (1948).

[23] G. Feinberg and J. Sucher, Phys. Rev. A **2**, 2395 (1970).

[24] R. Balian and B. Duplantier, Ann. Phys. (N.Y.) **112**, 165 (1978).
[25] H. Gies, K. Langfeld, and L. Moyaerts, J. High Energy Phys. 06 (2003) 018.
[26] H. Gies and K. Klingmüller, Phys. Rev. D **74**, 045002 (2006).
[27] H. Gies and K. Klingmüller, Phys. Rev. Lett. **97**, 220405 (2006).
[28] A. Bulgac, P. Magierski, and A. Wirzba, Phys. Rev. D **73**, 025007 (2006).
[29] T. Emig, R. L. Jaffe, M. Kardar, and A. Scardicchio, Phys. Rev. Lett. **96**, 080403 (2006).
[30] M. Bordag, Phys. Rev. D **73**, 125018 (2006).
[31] T. Emig and R. Büscher, Nucl. Phys. **B696**, 468 (2004).
[32] O. Kenneth and I. Klich, Phys. Rev. Lett. **97**, 160401 (2006). See also arXiv:0707.4017.
[33] T. Emig, A. Hanke, R. Golestanian, and M. Kardar, Phys. Rev. Lett. **87**, 260402 (2001).
[34] R. Büscher and T. Emig, Phys. Rev. Lett. **94**, 133901 (2005).
[35] R. P. Feynman and A. R. Hibbs, *Quantum Mechanics and Path Integrals* (McGraw-Hill, New York, 1965).
[36] See, for example, L. Schiff, *Quantum Mechanics* (McGraw-Hill, New York, 1968), 3rd ed..
[37] R. L. Jaffe, Phys. Rev. D **72**, 021301 (2005).
[38] Our result agrees with the one obtained by using the Abel-Plana formula in A. Romeo and A. A. Saharian, J. Phys. A **35**, 1297 (2002).
[39] A. R. Edmonds, *Angular Momentum in Quantum Mechanics* (Princeton University, Princeton, NJ, 1960).
[40] I. S. Gradshteyn and I. M. Ryzhik, *Tables of Integrals, Series, and Products* (Academic, New York, 1965).